Resistance to 5-aza-2'-deoxycytidine in Genic Regions Compared to Non-genic Repetitive Sequences

DNA

CONTENTS

GENERAL INTRODUCTION

General Introduction

Epigenetics is defined as heritable changes in phenotype or gene expression that does not involve changes in DNA sequence. Emergence of epigenetics provides explanation on various biological phenomena which could not be explained by genetic principles. An example of the epigenetic event is cellular differentiation, in which a vast majority of cells with identical genotype could give rise to a diversity of cell types with distinct cellular functions. Other epigenetic phenomena include imprinting of specific paternal or maternal loci in mammals (certain genes are expressed in a parent-of-origin-specific manner) and position effect variegation in the fruit fly Drosophila (in which the local chromatin environment of gene determines its expression).

In mammals, epigenetic mechanisms involve covalent modifications in DNA and in nucleosome, a fundamental chromatin unit which is composed of eight core histones (H3, H4, H2A, H2B) around which 147 base pairs of DNA are wrapped. DNA methylation comprises of attachment of a methyl group onto the fifth position of the cytosine ring of DNA, which occurs almost exclusively on CpG dinucleotide. DNA methylation is mediated by DNA methyltransferases (Dnmt). Several kinds of Dnmt have been discovered, and each Dnmt has preference on certain genomic regions (Hattori et al. 2004b). Heavily methylated DNA is associated to gene silencing. Histone modification refers to covalent modification of the amino acid residues of histone N-terminal tails which involves methylation, acetylation, phosphorylation, ubiquitylation, sumoylation, ADP ribosylation, deimination and proline isomerization (Kouzarides 2007). Functional effects of histone modification depend on the position of

the modified amino acid residue and also types of the modification. For instance, histone 3 lysine 9 (H3K9) methylations are usually found in heterochromatic regions whereas histone 3 lysine 4 (H3K4) methylation and histone 3 acetylation are associated with active transcription (Fig. GI-1).

Epigenetic modifications are dynamic and changeable throughout the life span. *Oct-4*, a stem cell marker, has a low DNA methylation level and a high histone acetylation level in undifferentiated cells. When cells differentiate, it becomes heavily methylated and silenced (Hattori et al. 2004). Aberrant epigenetic modifications or epimutations, result in various diseases. Heavy methylation in tumor suppressor genes or demethylation in oncogenes associates with cancer. Abnormal methylation in imprinting control regions caused deregulation of imprinting and chromosomal instability that leads to Fragile X syndrome and ICF syndrome (Warren et al. 2007; Matarazzo et al. 2009). Epimutations are further complicated with diverse relationships between DNA methylation and histone modifications, contributing to the varieties of epigenetic disorder.

By reversing the aberrant epigenetic modifications to their original states, epigenetic therapy provides treatment options for epigenetic disorders. Many agents that alter methylation patterns on DNA or the modifications of histones have been discovered, and some of these agents have recently been approved for cancer treatment (Table GI-1). One of these, 5-aza-2'-deoxycytidine (5azadC), have shown promising response rate in patients with myelodysplastic syndrome and chronic myeloid leukemia along with a reversal of p15 hypermethylation in bone marrow (Hackanson et al. 2005). Although the

epigenetic drugs could reverse epigenetic status of target genes, possibility to disturb balance of the other epigenetic modifications, remains a doubt.

In this thesis, I addressed questions regarding the effect of 5azadC, a DNA methyltransferase inhibitor, on different genomic regions. In Chapter 1, I investigated the epigenetic effect of 5azadC on non-genic repetitive sequences and genic regions. Studies in Chapter 2 focused on the role of DNA methylation and histone modifications in controlling *Tgfbi*, a gene associated in corneal development, and the possible mechanisms involved in resistance of genic regions to 5azadC. Understanding the epigenetic mechanisms allows proper use of the epigenetic drug in treating *Tgfbi* associated disorders.
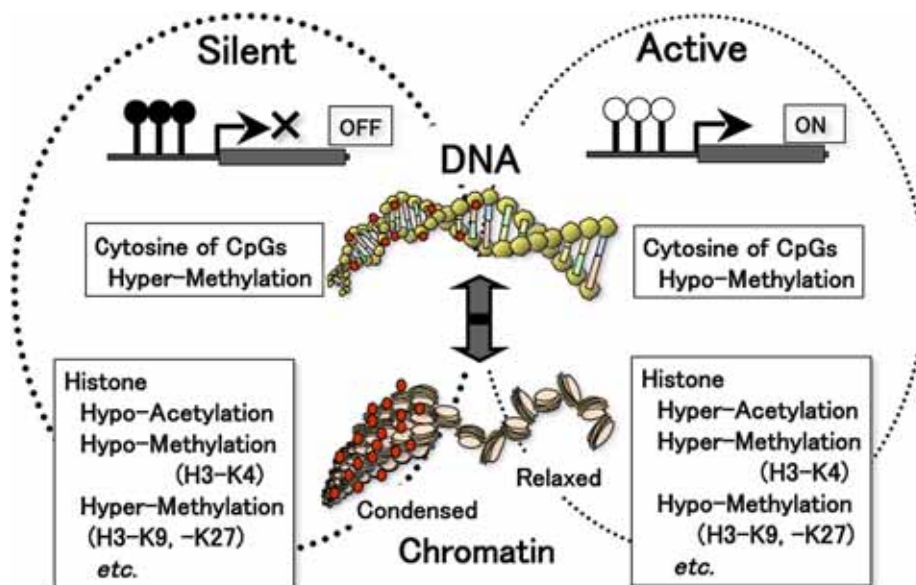
Figure GI-1. DNA methylation and histone modifications in epigenetic mechanisms. Both DNA methylation and histone modification regulate gene expression. Hypermethylation in CpG sites is associated with gene silencing whereas actively transcribed genes have hypomethylated CpGs. Condensed chromatin states which contain less acetylation and histone H3K4 methylation but high level of H3K9 and H3K27 methylations are transcriptionally inaccessible and vice versa (Adapted from Ohgane et. al 2008).

Table GI-1. Epigenetic drugs used in the clinic.

Drug name	Cancer
DNA methylation inhibitors	
5-azacytidine (FDA approved)	MDS, AML, CML
5-aza-2'-deoxycytidine (FDA approved)	AML, CML, MDS
MG98	Renal cell carcinoma
RG108	Colon cancer cell line
Procainamide	Colon cancer cell line
HDAC inhibitors	
SAHA (FDA approved)	CTCL, various solid tumors
PXD101	Various solid tumors
LBH589	CTCL
Depsipeptide	Multiple cancer cell lines, MDS, AML
Phenylbutyrate	MDS
Valproic acid	Neuroblastoma cells
MS-275	Prostate cancer cell lines, various solid tumors and lymphoid malignancies
Cl-994	Various solid tumors

FDA, Food and Drug Administration; MDS, myelodysplastic syndrome; AML, acute myeloid leukemia; CML, chronic myeloid leukemia; HDAC, histone deacetylase; SAHA, suberoylanilide hydroxamic acid; CTCL, cutaneous T-cell lymphoma. (Adapted from Cortez and Jones 2008).

CHAPTER 1

Resistance to 5-aza-2'-deoxycytidine in Genic Regions Compared to Non-genic Repetitive Sequences

Introduction

DNA methylation is one of the epigenetic events associated with gene regulation and function. Hypermethylation of promoter regions of tumor suppressor genes causes silencing of the genes that lead to cancer (Herman et al. 1998; Esteller et al. 1999; Tessema et al. 2003). Thus, reversing the methylation status of gene promoters to their prevalent methylation states has become a treatment option for certain cancer types. To date, there are many types of demethylating agents that have been shown to inhibit promoter methylation and reactivate silenced genes (Creusot et al. 1982; Villar-Garea et al. 2003; Cheng et al. 2004). Some of these have been approved or are in clinical studies to be developed as cancer drugs (Cortez & Jones, 2008).

5-aza-2'-deoxycytidine (5azadC), also known as decitabine, has been widely used as a DNA methyltransferase (Dnmt) inhibitor to reverse aberrant hypermethylation (Daskalakis et al. 2002; Zhu et al. 2001). It has been approved for hematological malignancies, showing favorable results with low dose treatment (Issa et al. 2004; Jabbour et al. 2008). Known to have dual modes of action, 5azadC at low doses induces gene hypomethylation, whereas high doses of 5azadC induce cytotoxicity and cause severe side effects in patients (Lima et al. 2003; Oki et al. 2007).

Nearly 40% of the mouse genome is composed of repetitive sequences including different classes of interspersed repeats such as LINEs, SINEs, LTR elements and satellites which are mainly found in heterochromatin regions (Waterston et al. 2002). Most repeats are densely methylated, and methylation in repeats reflects the global

methylation level (Yang et al. 2004; Jeong et al. 2005). Loss of methylation in repeats causes genomic instability (Ji et al. 1997; Weber & Schubeler 2007). Conversely, genes comprise only a small portion of the genome. Tissue-dependent and differentially methylated regions (T-DMRs) are unique sequences in genic regions which are methylated depending on tissue or cell types. The T-DMRs are widely observed, including in undifferentiated embryonic stem cells, normal tissues and even in cloned mice (Shiota et al. 2002; Hattori et al. 2004a; Ohgane et al. 2004; Yagi et al. 2008). Both repetitive regions and T-DMRs serve as important markers for methylation analysis, as the repeats could be used to estimate global methylation, whereas T-DMRs could serve as references for cell- or tissue-specific methylation.

Reports show that Dnmts have functional cooperation on genomic regions (Liang et al. 2002; Chen et al. 2003). We reported previously that Dnmt1, Dnmt3a and 3b share targets in the same CpG islands with T-DMRs, and each Dnmt has target preferences depending on the genomic regions (Hattori et al. 2004b). Dnmt3a and 3b prefer T-DMRs of genic regions, whereas Dnmt1 prefers repetitive sequences.

5azadC exerts its demethylating effect by binding to Dnmts (Creusot et al. 1982). Since Dnmts have multi targets, when using 5azadC, there is the potential of having a genome-wide demethylating effect. Demethylation of non-targeted genomic regions might occur, not only in cancer cells but also in normal cells. In addition, there are diverse interactions between DNA methylation and histone modifications in euchromatic and heterochromatic regions (Lachner & Jenuwein 2002; Vermaak et al. 2003). It may be possible to induce hypomethylation-independent activation of gene

expression and downstream responses. To know whether 5azadC induce invariable effect on different genomic regions, we investigated the effect of 5azadC on non-genic repetitive sequences and some genic regions including T-DMRs in fibroblast cells.

Materials and Methods

Reagents, cell culture and genome extraction

All reagents were purchased from Wako Pure Chemicals (Osaka, Japan) unless stated otherwise.

NIH/3T3 cells were cultured in Dulbecco's modified Eagle's medium (DMEM; Invitrogen, Carlsbad, USA) supplemented with 10% fetal bovine serum (JRH, Lenexa, USA) and 50 unit/ml penicillin / 50 μg/ml streptomycin (Invitrogen) at 37°C, 5% CO_2 in air. Prior to treatment with 5-aza-2'-deoxycytidine (5azadC; Sigma-Aldrich, Missouri, USA; diluted with sterile water to concentrations required), cells were plated at 1×10^5 cells/150 mm dish and cultured for 24 hr. Cells were treated with 5azadC to final concentrations ranging from 0.001 to 5 μM. 5azadC was substituted with sterile water in the untreated control. Medium was changed every 24 hr, and cells were collected after 3 days for DNA extraction.

Wild type ES cells (J1) and mutant ES cells deficient of *Dnmt1* (*Dnmt1*$^{-/-}$; c/c) and *Dnmt3a*, *3b* (*Dnmt3a*$^{-/-}$*3b*$^{-/-}$; 7aabb) were cultured on gelatin coated dishes with ES medium containing 1000 U/ml leukemia inhibitory factor (Chemicon, Temecula, USA) as previously described (Hattori et al. 2004b). J1, c/c and 7aabb cells were harvested at passage numbers 32, 17 and 17, respectively.

Cells were incubated in lysis buffer (150 mM EDTA, 10 mM Tris-HCl, pH 8.0 and 1% SDS) containing 10 mg/ml proteinase K (Merck, Darmstadt, Germany) at 55°C for 20 min. Following phenol/chloroform/isoamyl alcohol extraction twice, genomic DNA was precipitated with ethanol and was dissolved in TE buffer (10 mM Tris-HCl, 1 mM EDTA, pH 8.0).

Cell proliferation assay

NIH/3T3 cells were seeded into 96-well plates at 1×10^3 cells per well, 24 hr before 5azadC was added. Cells were treated with 5azadC at final concentrations of 0 (as control), 0.001, 0.005, 0.01, 0.05, 0.1, 0.5, 1.0, 5.0 and 10.0 μM for 3 or 4 days at 37°C, 5% CO_2 in air with medium changes every 24 hr. Four hours before plate reading, 10 μl of Cell Proliferation Reagent WST-1 (Roche, Penzberg, Germany) was added. Absorbance of each sample was measured against a background control using an ELISA reader at 450 nm absorption wavelength.

Analysis of the methylation status of repetitive sequences by Southern blotting

Genomic DNA (5 μg) was digested with restriction enzyme *Msp*I (Takara, Kyoto, Japan) or *Hap*II (Takara) and was electrophoresed on a 0.8% agarose gel. Following hydrolyzation with 0.25 N HCl and denaturation with 1.5 M NaCl/0.5 N NaOH, DNA was transferred onto nylon membrane. The membrane was probed with pMO for endogenous C-type retrovirus (MoMuLV) (Genebank accession NC_001501) and pMR150 for minor satellite repeats (X14469 and X07949). Probes were labeled with Gene Images random prime labeling module (Amersham Pharmacia, UK). Hybridization and detection were performed using Gene Images CDP-star detection module (Amersham Pharmacia) according to the manufacturer's instructions.

Bisulfite restriction mapping and sequencing

Genomic DNA, digested with *Eco*RI, was denatured by incubating with 0.3 M NaOH at 37°C for 15 min. Sodium metabisulfite (pH 5.0) and hydroquinone were added to a final concentration of 2 M and 0.5 mM respectively, and the mixture was incubated

at 55°C for 18 hr in the dark. Bisulfite modified DNA was purified with the Wizard

DNA Clean-up System (Promega, Madison, US), and the bisulfite reaction was

terminated with NaOH at a final concentration of 0.3 M at 37°C for 15 min. Sample was

neutralized by adding NH_4OAc, pH 7.0 (3 M, final concentration) and was precipitated

with ethanol. Purified DNA was dissolved in sterile water, and was amplified using

Immolase (BIOLINE, Tokyo, Japan) with primer sets as follows: ODE F,

5'-TAAGGGTAGGTATATAGGTGTGGT-3' and R,

5'-TCTACCCCCTTTAAAAATCACTTTAA-3'; OPR F,

5'-TGGGTTGAAATATTGGGTTTATTT-3' and R,

5'-CTAAAACCAAATATCCAACCATA-3'; *Per1* F,

5'-GGGAAGGGGATTTTGTTATTGTAGT-3' and R,

5'-CATAAACCCAACAACAAACCCATCT-3'; *Sall3* F,

5'-GTTAGGGTTTTTTTAG-GGTATTAGT-3' and R,

5'-CCCTAATCTACCCAACATATACAAA-3'. The PCR conditions were as follow:

95°C for 10 min, followed by 40 cycles of denaturation at 94°C for 30 sec, annealing at

55°C for 30 sec, and extension at 72°C for 1 min, and a final extension at 72°C for 10

min.

 Oct-4 distal enhancer, *Oct-4* proximal enhancer and promoter PCR products were

digested with *Taq*I (Takara) at 65°C and *Per1* and *Sall3* PCR products were digested

with *Hpy*CH4IV (NEB, Ipswich, MA) at 37°C for 3hr. Restricted fragments were

assessed by agarose gel electrophoresis. Images were recorded and semiquantified using

ImageJ software provided by National Institutes of Health (http://rsbweb.nih.gov/ij/).

Relative DNA methylation level of each genic region was calculated by the formula:

DNA methylation status (%) $= 100 \times I^C / (I^{UC} + I^C)$ where I^C and I^{UC} represent the

intensities of the digested and undigested bands, respectively.

For bisulfite sequencing, PCR products were cloned into pGEM T-Easy vector (Promega, Madison, USA), and 10 clones were sequenced for each sample. Primer sets used were: *Oct-4* F, 5'- TGGGCTGAAATACTGGGTTCACCC-3' and R, 5'-CTGAAGCCAGGTGTCCAGCCATG-3'; *Dpep1* F, 5'-GGTTGGGGAATTGGTTGTT-3' and R, 5'-CAACCTACTCCTAAATCCTCCA-3'; *Clu* F, 5'- TAGTGAGTGGGGATGTAGTATTATGG-3' and R, 5'-AACCCCTAAACAACTTCAAAATTTT-3'; *Igf2r* F, 5'-GTTTAGAATATTGGTGAGTAGTGGG-3' and R, 5'-CCTTAAAATAAAAATAAACATCTTAAA-3', with following PCR conditions: 95°C for 10 min, followed by 40 cycles of denaturation at 94°C for 30 sec, annealing at 55°C for 30 sec, and extension at 72°C for 1 min, and a final extension at 72°C for 10 min.

RNA extraction and RT-PCR

Total RNA was extracted with TRIzol reagent (Invitrogen) according to the manufacturer's instructions. First strand cDNA was synthesized with SuperScript™ III First-Strand Synthesis System for RT-PCR (Invitrogen), and RT-PCR was performed using Taq DNA Polymerase (Promega) with primers as follows: *Dnmt1* F, 5'-CAGGAGTGTGTGAGGGAG-3'; R, 5'-GGTGTCACTGTCCGACTTGC-3'; *Dnmt3a* F, 5'-ACCCATGCCAAGACTCACCTTC-3'; R, 5'-TCCACCTTCTGAGACTCTCCAG-3'; *Dnmt3b* F, 5'-TCAGACACGAAGGATGCTCC-3'; R, 5'-ACAGGGTACTCCTGCACATG-3'; *β-actin* F, 5'-TTCTACAATGAGCTGCGTGTGG-3'; R,

5'-ATGGCTGGGGTGTTGAAGGT-3'; *Oct-4* F-5'-GGCGTTCGCTTTGGAAAGGTGTTC-3'; R, 5'-CTCGAACCACATCCTTCTCT-3'; *Clu* F, 5'- CCAGTCGAAGATGCTCAACA-3'; R, 5'- TGTGATGGGGTCAGAGTCAA-3'; *Dpep1* F, 5'-ATGCGGTATCTGACCCTCAC-3'; R, 5'- ATCTGCAAAGCGTCCTTCAT-3'; *Igf2r* F, 5'- CAACGTCTGTGGAAATGTGG-3'; R, 5'- CAGCCCATAGTGGTGTTGAA-3'. PCR conditions were as follow: 95°C for 1 min, followed by 30 cycles of denaturation at 94°C for 30 sec, annealing at 60°C for 30 sec, and extension at 72°C for 1 min, and a final extension at 72°C for 5 min.

Chromatin immunoprecipitation (ChIP) assay

ChIP assays were performed as described previously (Hattori et al. 2004b) using a Chromatin Immunoprecipitation (ChIP) Assay Kit (Cat. No. 17-295; Upstate Biotechnology, Lake Placid, NY), with anti-acetylated histone H3 and H4 antibodies (Cat. No. 06-599 and 06-598; Upstate Biotechnology), anti-trimethylated H3K4 and H3K9 (Cat. No. ab8580 and ab8898; Abcam, Cambridge, UK), and anti-dimethylated H3K4, H3K9 and H3K27 (Cat. No. 07-030, 07-212 and 07-452; Upstate Biotechnology). Normal rabbit IgG (Cat. No. 12-370; Upstate Biotechnology) was used as a negative control to verify immunoprecipitation specificity. PCR was performed using primers as follows: *Oct-4* F, 5'- GTGAGGTGTCCGGTGACCCAAGGCAG-3' and R, 5'- CGGCTCACCTAGGGACGGTTTCACC-3'; *Clu* ChIP 1 F, 5'-TGCTCTGGAGACACAGGAAA-3' and R, 5'- CTGGGGAAGAAAGCCAAGAT-3'; *Clu* ChIP 2 F, 5'- ATTGCAGTGATGCCAGATGA-3' and R, 5'- ACGCACAGCAGGAGAATCTT-3'; *Dpep1* F, 5'-CTCCTCTTGTGGCTCCCTAA-3'

16

and R, 5'-GGCTCCACAGAGTGCCAAG-3', with following PCR conditions 95°C for 10 min, followed by 30 cycles of denaturation at 94°C for 30 sec, annealing at 55°C for 30 sec, and extension at 72°C for 1 min, and a final extension at 72°C for 10 min. Amount of each PCR product on an ethidium bromide stained gel-image was evaluated using ImageJ software.

Results

Demethylating effect of 5azadC on repetitive sequences

We examined cell survival under different concentrations of 5azadC by WST-1 assay. After 72 hr, viable cell number was largely reduced at concentrations at and higher than 0.5 μM, and was severely affected at higher concentrations (Fig. 1A). A similar effect was observed in the 96 hr culture. Only minimal effects on viability were observed on cells treated with less than 0.1 μM 5azadC.

To determine the effect of 5azadC on the methylation of repetitive sequences, cells were treated with 0.001 μM to 5 μM 5azadC, and the methylation status of repetitive sequences was analyzed using methylation-sensitive restriction enzymes. Southern hybridization was performed using two probes of differentially localized repetitive sequences, minor satellite repeats which are located in the centromeric regions and endogenous C-type viruses which are interspersed across the mouse genome (Joseph et al. 1989; Waterston et al. 2002; Hattori et al. 2004b). Minor satellite repeats were demethylated extensively starting at the 0.1 μM concentration (Fig. 1B), and 1 μM was sufficient to induce a maximum demethylating effect. Similarly, endogenous viruses showed aggressive loss of methylation at 0.1 μM to 5 μM treatment levels, but slight demethylation could be observed at a concentration as low as 0.001 μM. Thus, the repetitive sequences were strongly demethylated by 5azadC. The results confirmed previous report that 5azadC is effective in inducing demethylation dose-dependently from 0.1 μM to 5 μM (Davidson et al. 1992).

Effect of 5azadC on genic regions

We next examined the effect of 5azadC on T-DMRs of genic regions. *Oct-4* (*Pou5f1*) has T-DMRs in the CpG rich promoter/proximal enhancer region and the distal enhancer region (Fig. 1-2A; Hattori et al. 2004a). DNA methylation status of the T-DMRs was analyzed using bisulfite restriction mapping focusing on *Taq*I restriction sites. At 0.001 and 0.01 μM 5azadC, methylation levels of the investigated regions had changed little compared to the untreated ones (Fig. 1-2B&C). A significant loss of methylation in both regions was observed at 0.1 μM, indicating that this concentration was able to induce demethylation in both genic regions and the repetitive sequences. In the 1 and 5 μM treated samples, however, both T-DMRs had nearly the same methylation levels as in the untreated control, in contrast to the extensive demethylation observed in the repetitive sequences at these concentrations.

Sall3 has a T-DMR located at an edge of a CpG island, which is methylated in trophoblast cell lineage (Shiota et al. 2002; Ohgane et al. 2004). The T-DMR is aberrantly methylated in the placental genome of cloned mice (Ohgane et al. 2004). *Per1*, which is involved in generating circadian rhythm, has a few CpGs at the upstream promoter region. Similar to *Oct-4*, 0.001 and 0.01 μM 5azadC had minimal effects on these loci. Methylation levels decreased significantly following 0.1 μM 5azadC treatment, but were only slightly decreased at 1 μM, and remained unchanged at 5 μM.

Bisulfite sequencing was performed on several gene loci containing CpG rich promoters, including *Oct-4*. Hypomethylation of the *Clusterin* (*Clu*) promoter is associated with high gene expression in rat testis and epididymis (Rosemblit et al. 1994).

Dpep1, a renal *Dipeptidase* gene, has been reported as a tumor marker candidate in malignancies (McIver et al. 2004). All investigated loci had hypermethylated promoter regions in NIH/3T3 cells (Fig. 1-3A). Bisulfite sequencing results on the *Oct-4* promoter region validated the restriction mapping results that 0.1 µM was more effective in inducing demethylation in genic regions compared to 1 µM. Similar dose-dependent demethylation patterns were also observed in the promoter regions of *Clu* and *Dpep1*.

We also analyzed DMR2 region of the *Igf2r* imprinted gene, which is differentially methylated depending on its parental origin (Stoger et al. 1993). Due to allele specific methylation, half of the clones were methylated in the untreated control. As observed in other genes, the DMR2 region appeared demethylated at 0.1 µM, but was not affected by 1 µM 5azadC.

These results provide evidence that 5azadC has a strong demethylating effect on repetitive sequences, but its effect on genic regions is limited to a certain effective dose. The expression levels of *Dnmt1*, *Dnmt3a* and *Dnmt3b* were not affected by 5azadC at concentrations from 0.001 to 5 µM (Fig. 1-3B), indicating that partial retention of methylation observed at high concentrations of 5azadC was not due to increased Dnmt expression.

5azadC induced a unique combination of histone tail modifications

Since 0.1 and 1 µM 5azadC showed rather unexpected, different demethylation effects on genic regions, we investigated changes in histone modifications by

performing ChIP assay with antibodies against euchromatic and heterochromatic marks. The AcH3 level in genic regions continuously declined as concentration of 5azadC was increased (Fig. 1-4A), which is in contrast to the condition in decondensed chromatin (Vermaak et al. 2003). Such changes were not observed in AcH4, which was less enriched in genic regions.

Both H3K4me2 and H3K4me3 levels increased with 5azadC treatment, in almost all investigated regions, and high levels were correlated with increased gene expression (Fig. 1-4B). Elevation of H3K4me2 in *Dpep1* at 1 μM 5azadC corresponded to a remarkable transcriptional increase, and the relatively low abundance of H3K4me2 in *Oct-4* promoter region at any level of 5azadC did not induce *Oct-4* expression. H3K4me3 was more enriched by 0.1 μM than by 1 μM 5azadC treatment.

Heterochromatin-associated H3K9me2 and H3K27me2 marks continuously decreased with 5azadC treatment. In contrast, elevation of H3K9me3 was observed, with higher enrichment at 1 μM compared to 0.1 μM 5azadC in most regions. Altogether, 5azadC treatment at different concentrations was accompanied by a distinct combination of changes in euchromatic and heterochromatic histone marks in genic regions.

Increase of H3K9me3 correlates with partially methylated regions

Studies show that H3K9 methylation directs DNA methylation (Jackson et al. 2002; Tamaru et al. 2001). To date, our data showed that 5azadC induces partial demethylation, not complete demethylation in genic regions. To find out whether increased H3K9me3

21

is associated with DNA methylation, we investigated enrichment of H3K9 methylation in *Dpep1* and *Clu* promoter regions in Dnmt deficient cells. The promoter region of *Dpep1* and *Clu* was heavily methylated in wild type ES cells, and was demethylated in *Dnmt1*^{-/-} and in *Dnmt 3a*^{-/-}*3b*^{-/-} (Fig. 1-5A). Increase of H3K9me3 at the genic regions in Dnmt knock out cells was not obvious as those in 5azadC treated NIH/3T3 cells (Fig. 1-5B). Therefore, increased H3K9me3 correlated with partially methylated regions, for instance, in 5azadC treated cells. Similar to 5azadC treated cells, H3K9me2 decreased in *Dnmt1*^{-/-} cells, but was increased in *Dnmt3a*^{-/-}*3b*^{-/-} cells.

Discussion

Current results demonstrate that 5azadC has differential effects on non-genic repetitive sequence and genic regions (Fig. 1-6). Importantly, non-genic repetitive sequences are susceptible to 5azadC, whereas genic regions are only demethylated by effective low doses. Therefore, several issues are raised regarding the use of 5azadC.

Genic regions were only demethylated at effective concentrations, but not at higher concentrations. Demethylation of repetitive sequences was concentration dependent. Thus, increasing treatment dosage might not effectively induce demethylation in targeted genic regions, but will lead to genome-wide hypomethylation in non-cancer cells. Loss of methylation promotes additional genomic changes, including increased mutation rate and pericentromeric rearrangement (Ji et al. 1997; Chen et al. 1998). Thus, before using 5azadC for cancer treatment, precise doses should be determined to achieve localized hypomethylation in cancer cells, but avoid concurrent global hypomethylation in normal cells.

Some reports showed that 5azadC treatment is followed by decreased H3K9 di-methylation (Nguyen et al. 2002; Fahrner et al. 2002; Wozniak et al. 2007). Our results also showed decreased H3K9me2, but increased H3K9me3 at all genic regions after 5azadC treatment. H3K9me3, but not H3K9me2, is a mark for cytosine methylation in chromatin regions in *Neurospora crassa* (Tamaru et al. 2001). Thus, increased H3K9me3 might be associated with partial methylation in 5azadC treated

cells, indicating a functional difference between H3K9me2 and H3K9me3 in mammalian cells.

Unusual histone tail modifications were observed following 5azadC treatment, in contrast to their authentic roles in DNA methylation and gene silencing (Lachner & Jenuwein 2002; Vermaak et al. 2003). Such changes might reflect mechanisms to prevent full demethylation in genic regions. As DNA methyltransferases are associated with H3K9 methyltansferases (Fuks et al. 2003; Li et al. 2006), accumulation of histone methyltransferases, which confers increase in H3K9me3, may also attracts Dnmts. Recruitment of MeCPs to the methylated DNA region is associated with a co-repressor complex containing mSin3 and histone deacetylases (HDACs), causing reduction of AcH3 (Jones et al. 1998; Nan et al. 1998). Given that Dnmt1 has preference on repetitive sequence whereas Dnmt3a and 3b are in favor to gene regions (Hattori et al. 2004b), current study may reflect preference of 5azadC to Dnmt1 (Fig.1-6). Thus Dnmt3 might be associated with H3K9 methyltransferases for maintaining the methylation level in genic regions, due to the functional cooperation of Dnmt1 and Dnmt3 (Rhee et al. 2000; 2002; Hattori et al. 2004b).

Gene activation by 5azadC seems to involve complex mechanism of action, in addition to DNA demethylation (Fahrner et al.2002; Wozniak et al. 2007). We showed that genes were upregulated at 0.1 μM, and expressions were maintained or increased at 1 μM, despite higher DNA methylation levels observed at 1 μM. Although transcriptional activation could be explained by an increase of H3K4 methylation marks (Santos-Rosa et al. 2002), AcH3 concurrently decreased drastically. Interestingly,

H3K4me3 abundance was lower in the 1 μM treatment than 0.1 μM and was accompanied by DNA hypermethylation. A similar study on cancer genes suggested that histone modifications of demethylated genes do not fully recover to euchromatic states (McGarvey et al. 2006). Thus, gene activation by 5azadC seems to be more complex than the authentic model of epigenetic gene activation and silencing.

Although studies showed that toxicity of 5azadC treatment was not due to a demethylating effect (Juttermann et al. 1994), our results raise questions concerning the 5azadC-toxicity mechanism. Repetitive sequences were partially demethylated at 0.1 μM, and were extensively demethylated at 1 and 5 μM. Concurrent with demethylation, cell viability was minimally affected at 0.1 μM, but was retarded at 1 and 5 μM, reflecting that the induced cytotoxicity might be an effect of global demethylation in the repetitive sequences. In contrast, genic regions were hypomethylated at 0.1 μM, and were methylated at 1 and 5 μM 5azadC, probably as a resistance mechanism against cell death.

This study provides an explanation of the mechanisms behind the dual modes of action of the demethylating drug 5azadC. At low concentrations, the demethylating effect is potent in both repetitive and genic regions. At high concentrations, repetitive sequences are highly demethylated, which potentially leads to toxicity. DNA methylation in genic regions is less affected, which might be due to histone modification changes attempting to maintain the DNA methylation level. Thus for therapeutic use, an appropriate dose of 5azadC should be chosen wisely when it is administered to patients in order to achieve targeted gene recovery and to minimize side

effects on normal cells concurrently.

Figure 1-1

A

B

Ethidium bromide   **Minor satelite**   **Endogenous virus**
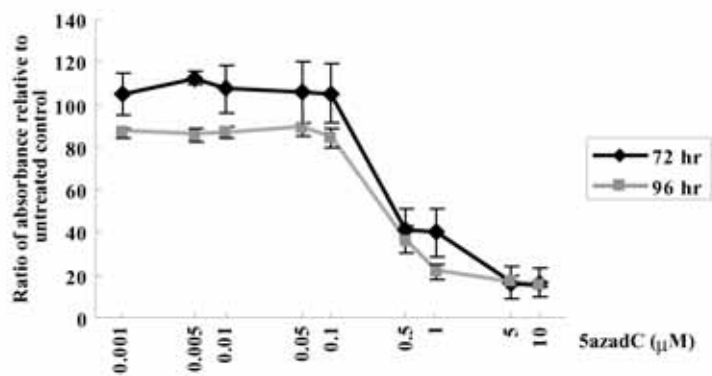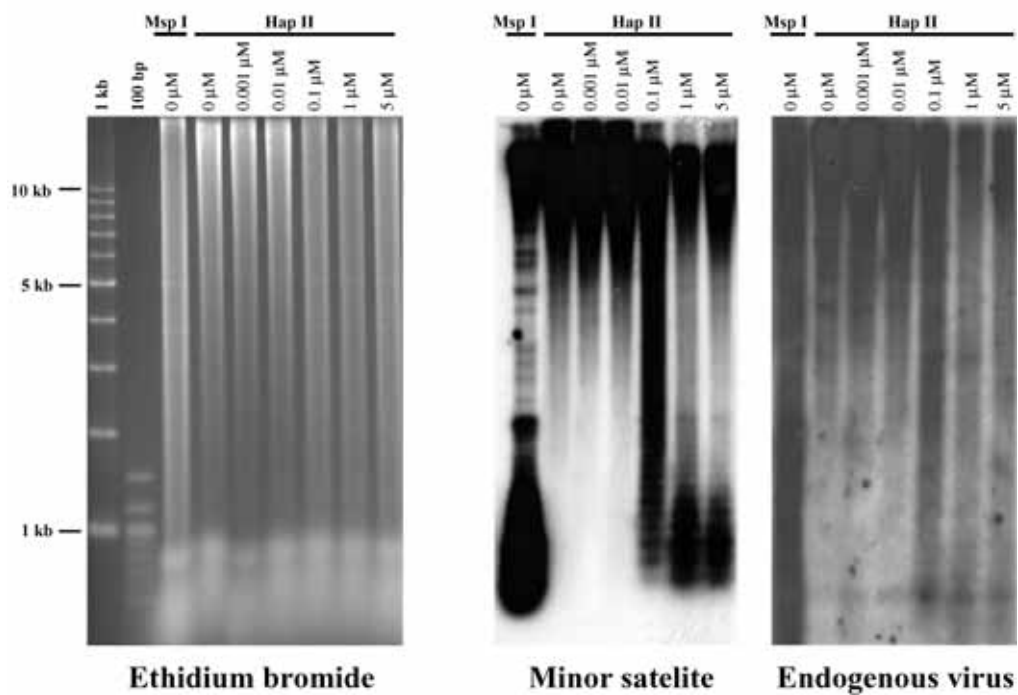
Figure 1-1. Demethylating effects of 5azadC on repetitive sequences.

A, **WST-1 cell proliferation assay was performed on cells treated with 5azadC at indicated concentrations for 72 and 96 hr.** Cell number was estimated by the absorbance, then represented as the ratio relative to the untreated control, the absorbance of which was arbitrarily set to 100.

B, **Analysis of the methylation status of repetitive sequences by Southern hybridization.** Genomic DNA (5 μg), digested with *Hap*II, was hybridized to probes for minor satellite repeats and endogenous viruses. As a control for complete digestion, DNA from the untreated control was digested with *Msp*I.

Figure 1-2

A

Oct-4

Sall3

Per1

B

5azadC (μM) 0 0.001 0.01 0.1 1 5

Oct-4 DE

Met (%)   43.9   51.6   57.4   34.6   51.5   49.2

Oct-4 PE/P

Met (%)   60.9   60.7   68.7   35.4   67.8   71.2

Sall3

Met (%)   90.0   77.2   71.2   60.1   49.6   100

Per1

Met (%)   25.2   23.1   22.6   3.2   9.4   24.3

◁ Uncut
◀ Cut

C

Oct-4 DE   Oct-4 PE/P   Sall3   Per1

0 μM
0.001 μM
0.01 μM
0.1 μM
1 μM
5 μM
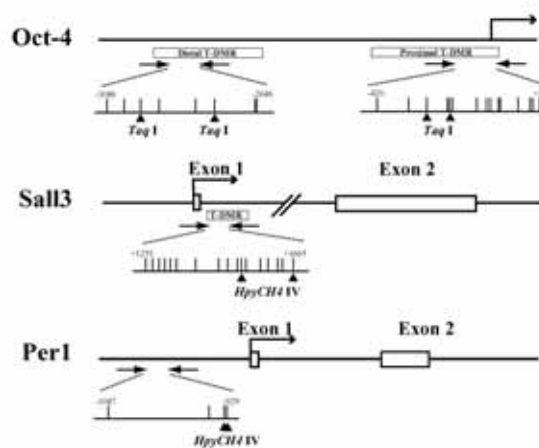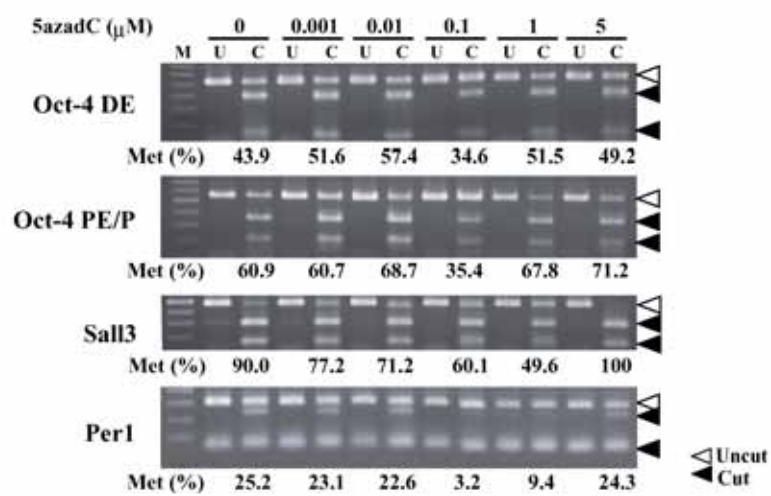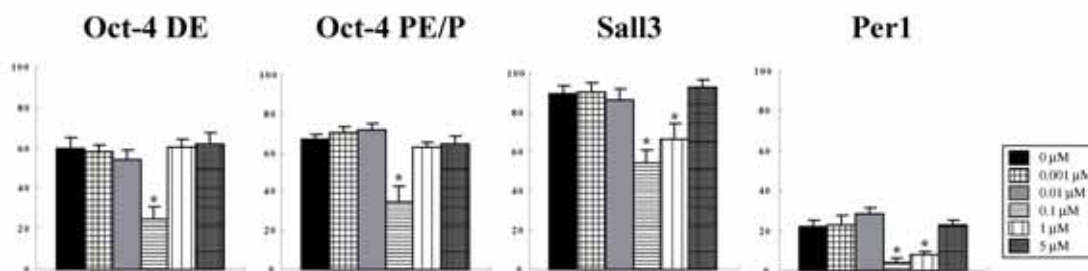
Figure 1-2. Methylation analysis of T-DMRs by bisulfite restriction mapping.

A, **Schematic diagram of T-DMRs.** T-DMRs are represented by bars and CG sites are represented by vertical lines. Locations of the amplified regions relative to each respective transcription start site are as follow: *Oct-4* distal enhancer (DE), -3086 to -2646; *Oct-4* proximal enhancer/promoter (PE/P), -420 to +31; *Sall3*, +1253 to +1665; *Per1*, -1087 to -929. Each locus contains 2 *Taq*I or *Hpy*CH4IV restriction sites, respectively (triangles).

B, **Restriction mapping.** PCR products were digested with restriction enzymes and electrophoresed on agarose gel. Relative DNA methylation level was calculated based on relative intensities of cut to uncut bands, indicated below each cut lane. M, marker; U, uncut; C, cut with restriction enzyme.

C, **Methylation level of T-DMRs.** Graph indicates methylation level of each gene locus at each concentration, represented by the means ± S.E. of 3 independent PCRs of 2 cultures. * $P<0.05$ (Student's t-test).

Figure 1-3

A
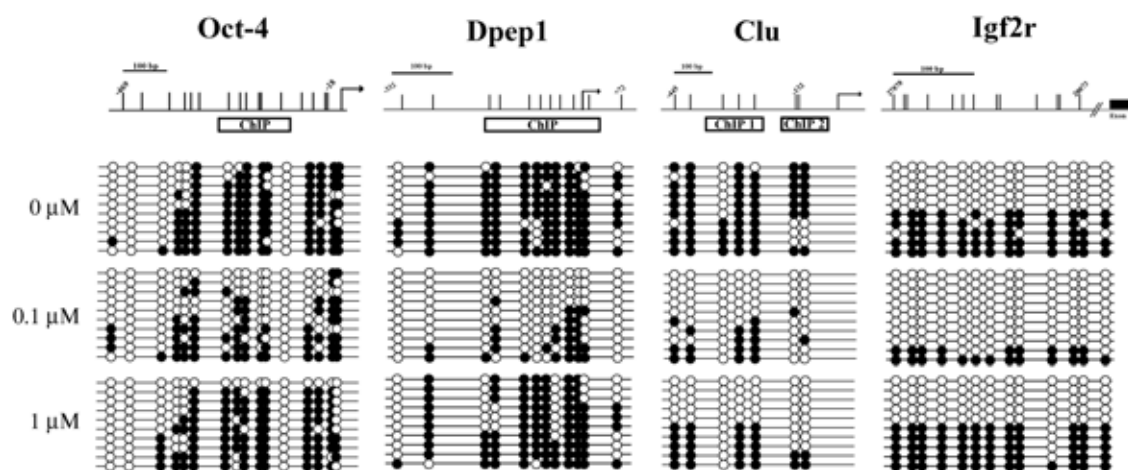
B
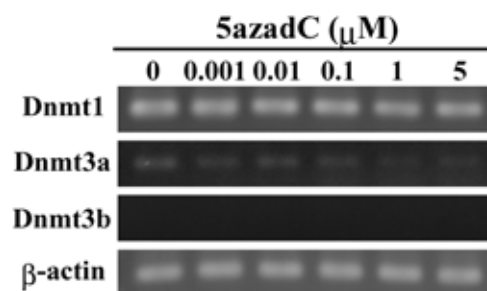
Figure 1-3. Methylation analysis of T-DMRs by bisulfite sequencing.

A, **DNA methylation analysis of 4 gene loci, *Oct-4*, *Clu*, *Dpep1* and *Igf2r*, using bisulfite sequencing.** Top panel shows location of individual CpG site (vertical lines) in genic regions amplified by PCR. The 0, 0.1 and 1 μM 5azadC treated DNA was bisulfite converted and sequenced. Methylation status of each CpG site is represented by open (unmethylated) or closed (methylated) circles.

B, **Expression of *Dnmt1*, *Dnmt3a* and *Dnmt3b* at 0 – 5 μM 5azadC analyzed by RT-PCR.** Expression level of β-actin was used as the internal control.

Figure 1-4

A

B
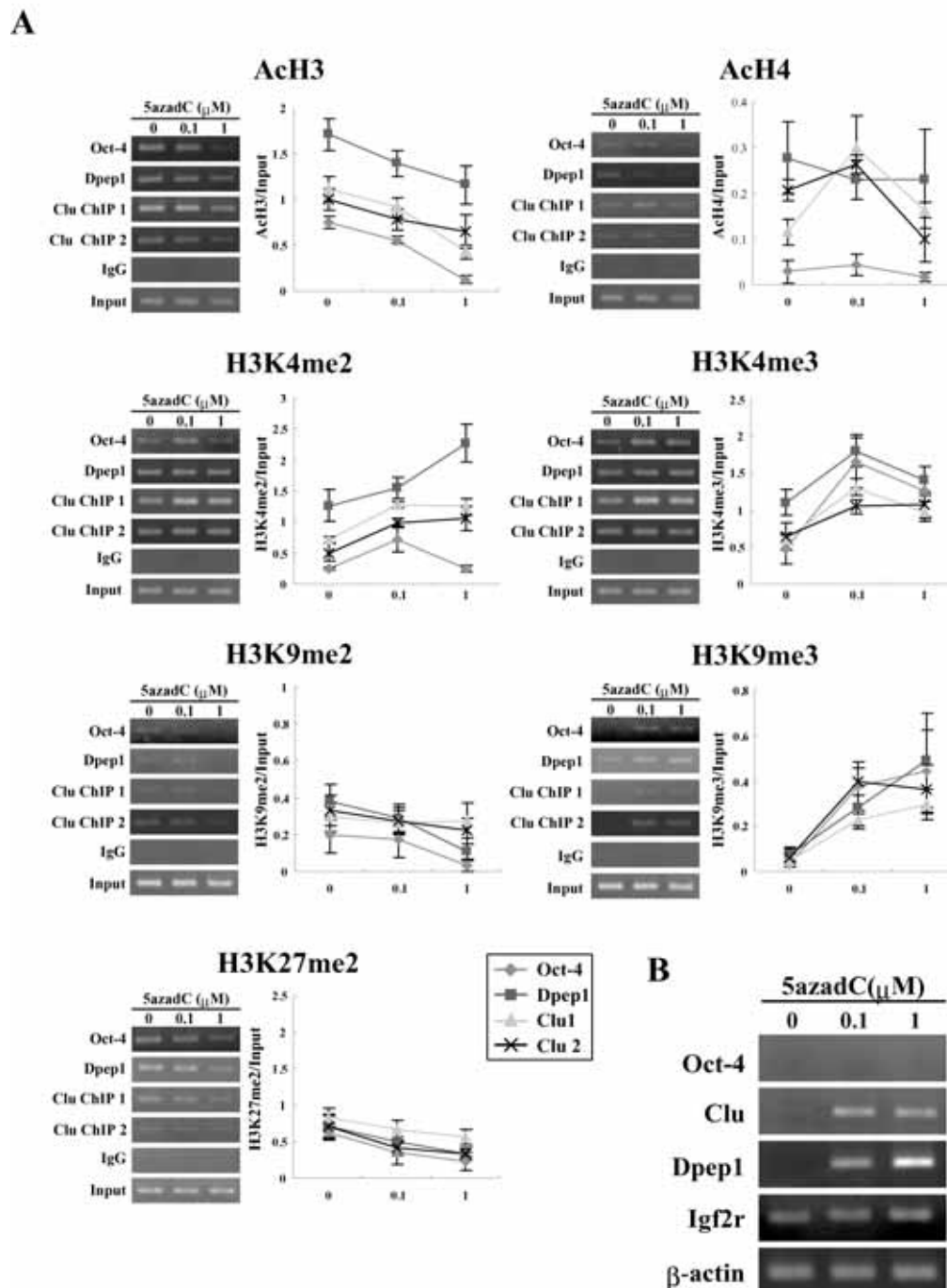
Figure 1-4. Histone modification status following 5azadC treatment.

A, **Histone modification analysis of 0, 0.1 and 1 μM 5azadC treated samples by ChIP.** Analyzed regions are indicated by boxed "ChIP" in the schematic diagram in Fig. 1-3A. DNA immunoprecipitated with respective antibodies was amplified by PCR and electrophoresed (left panels). Relative intensities of PCR bands to those of the input DNA, represented by the means ± S.E. of 3 independent PCRs of 3 cultures are shown in right panels.

B, **RT-PCR results of expression of each gene following 5azadC treatment.**

Figure 1-5

A

B
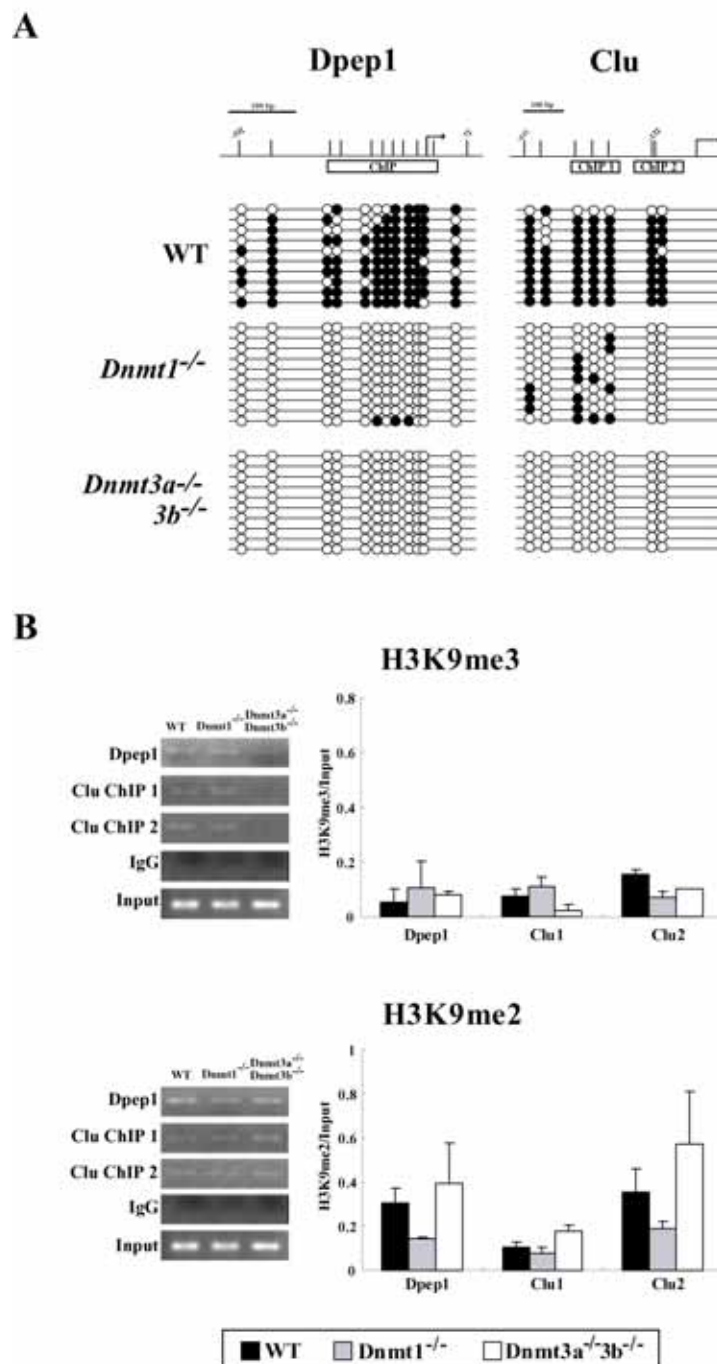
Figure 1-5. DNA methylation and H3K9 methylation status of *Dpep1* and *Clu* in Dnmt knock out ES cells.

A, **DNA methylation analysis of *Dpep1* and *Clu* by bisulfite sequencing.**

B, **Histone modification analysis.** H3K9 di- and tri-methylation levels at regions shown in panel *A* assessed by ChIP. Bar chart shows relative intensities of PCR bands to those of the input, represented by means ± S.E. of 3 independent PCRs of 2 cultures.

Figure 1-6
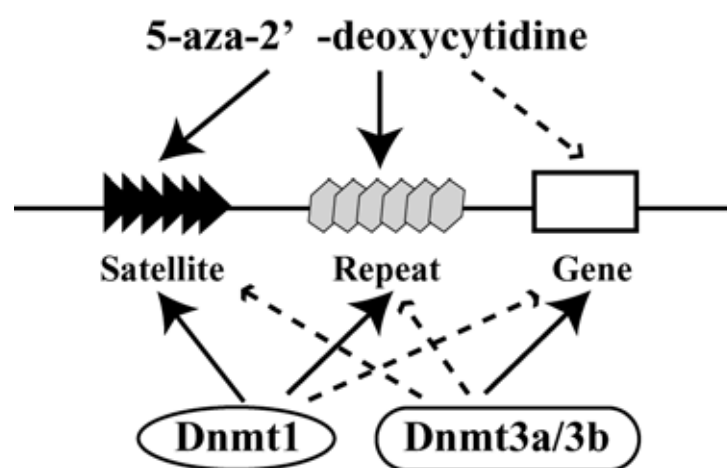
Figure 1-6. Summary of the effect of 5azadC on repetitive sequences and genic regions.

5azadC strongly demethylates repetitive sequences (black arrow) but only demethylates genic regions at low doses (dotted arrow). The study suggests the preference of 5azadC for Dnmt1, as Dnmt1 has a functional preference for repeats whereas Dnmt3a/3b functions on genic regions (Hattori et al. 2004b).

CHAPTER 2

Epigenetic Status of *Tgfbi* Gene

Introduction

Transforming growth factor beta-induced (*Tgfbi*) gene, also known as *Bigh3*, encodes keratoepithelin, which functions in wound healing and cell adhesion. It has a role in maintaining the integrity of normal cornea. Mutations in *Tgfbi* which occur mainly in 5q31 position of chromosome cause cornea deposits and different kinds of cornea dystrophies (Poulaki & Colby, 2008). *Tgfbi* is expressed in various tissues throughout mouse embryonic development and in different organs of transgenic mice, suggesting its multiple roles in biological regulations and functions (Schorderet et al. 2000; Bustamante et al. 2008).

Previously we identified genomic loci which are target loci of Dnmts by performing restriction landmark genomic scanning (RLGS) on Dnmt1 mutant ES cells and double mutant of Dnmt3a and Dnmt3b ES cells, using NotI as a landmark enzyme (Hattori et al. 2004b). These loci emerged as spots in the RLGS profiles of both Dnmt1-/- and Dnmt3a-/-3b-/- ES cells, indicating that they are common targets of both Dnmt1 and Dnmt3a/3b. The intensities of the spots were stronger in Dnmt3a-/-3b-/- ES cells compared to those in Dnmt1-/-, showing that the levels of demethylation are more extensive in Dnmt3a-/-3b-/- cells than in Dnmt1-/- cells. These implied that Dnmt3a and Dnmt3b primarily functions in methylating genic regions (Hattori et al. 2004b). *Tgfbi* had been identified as one of the target loci of Dnmts detected in RLGS (Hattori et al. 2004b).

Diverse covalent modifications at histone tails, known as the histone code, provide

signals for dynamic chromatic changes in between euchromatic and heterochromatic states (Strahl and Allis, 2000). Methylation of lysine 4 on histone H3 has been linked to transcriptional activation whereas lysine 9 methylation on histone H3, cause condensed chromatin structure and transcriptional silencing (Fig. GI-1). Evidences suggest the interplay between DNA methylation and histone modifications in controlling the chromatin states and gene expressions (Vermaak et al. 2003; Freitag & Selker, 2005). Changes in DNA methylation patterns in genomic regions, will cause changes in the histone modifications. Conversely, switching of the histone code also affects DNA methylation and chromatin structure.

Modifications on histone are catalysed by histone modifying enzymes. Numerous histone methyltransferases in the Suv39 subfamily of SET domain possess H3K9 catalytic activity, which include Suv39h1, Suv39h2, G9a, GLP/Ehmt1. Cells deficient in G9a methyltransferase causes reduction of DNA methylation in gene loci, retrotransposons and major satellite repeats (Ikegami et al. 2007; Dong et al. 2008). H3K9 trimethylation, mediated by histone methyltransferase DIM-5, is a mark for cytosine methylation in chromatin regions in *Neurospora crassa* whereas loss of function of H3K9 methyltransferase kryptonite causes depletion of cytosine methylation at sites of CpNpG trinucleotides (Tamaru & Selker, 2001; Jackson et al. 2002). These suggest the role of H3K9 histone methyltransferases in DNA methylation maintenance.

5azadC is commonly used in epigenetic research to reverse aberrantly methylated gene regions and to reactivate silenced genes. In similar manner, it has been used on tumor suppressor genes in cancer treatment. Despite promising results on treating

41

myelodysplastic syndrome, several concerns remain, mainly regarding the mechanisms and the effect of the drug. In Chapter 1, I showed the strong effect of 5azadC on non-genic repetitive sequences. The repetitive sequences became hypomethylated concentration dependently whereas genic regions were resistance to high concentrations of 5azadC. Changes in histone modification seemed to be involved to induce such resistance. To understand better of the role of histone modifications in demethylating resistance in genic regions, I studied the functional roles of Dnmts and histone methyltransferases on *Tgfbi* in Chapter 2.

Materials and Methods

Reagents, cell culture and genome extraction

All reagents were purchased from Wako Pure Chemicals (Osaka, Japan) unless stated otherwise.

NIH/3T3 cells were cultured in Dulbecco's modified Eagle's medium (DMEM; Invitrogen, Carlsbad, USA) supplemented with 10% fetal bovine serum (JRH, Lenexa, USA) and 50 unit/ml penicillin / 50 μg/ml streptomycin (Invitrogen) at 37°C, 5% CO_2 in air. Prior to treatment with 5-aza-2'-deoxycytidine (5azadC; Sigma-Aldrich, Missouri, USA; diluted with sterile water to concentrations required), cells were plated at 1×10^5 cells/150 mm dish and cultured for 24 hr. Cells were treated with 5azadC to final concentrations of 0.1 and 1 μM. 5azadC was substituted with sterile water in the untreated control. For TSA treatment, 200 nM of TSA (Sigma) were added using ethanol as carrier. Medium was changed every 24 hr, and cells were collected after 3 days for DNA extraction.

Wild type ES cells (J1) and mutant ES cells deficient of *Dnmt1* (*Dnmt1*$^{-/-}$; c/c) and *Dnmt3a*, *3b* (*Dnmt3a*$^{-/-}$*3b*$^{-/-}$; 7aabb) were cultured on gelatin coated dishes with ES medium containing 1000 U/ml leukemia inhibitory factor (Chemicon, Temecula, USA) as previously described (24). J1, c/c and 7aabb cells were harvested at passage numbers 32, 17 and 17, respectively.

Cells were incubated in lysis buffer (150 mM EDTA, 10 mM Tris-HCl, pH 8.0 and

1% SDS) containing 10 mg/ml proteinase K (Merck, Darmstadt, Germany) at 55°C for 20 min. Following phenol/chloroform/isoamyl alcohol extraction twice, genomic DNA was precipitated with ethanol and was dissolved in TE buffer (10 mM Tris-HCl, 1 mM EDTA, pH 8.0).

Bisulfite restriction mapping and sequencing

Genomic DNA, digested with *Eco*RI, was denatured by incubating with 0.3 M NaOH at 37°C for 15 min. Sodium metabisulfite (pH 5.0) and hydroquinone were added to a final concentration of 2 M and 0.5 mM respectively, and the mixture was incubated at 55°C for 18 hr in the dark. Bisulfite modified DNA was purified with the Wizard DNA Clean-up System (Promega, Madison, US), and the bisulfite reaction was terminated with NaOH at a final concentration of 0.3 M at 37°C for 15 min. Sample was neutralized by adding NH_4OAc, pH 7.0 (3 M, final concentration) and was precipitated with ethanol. Purified DNA was dissolved in sterile water, and was amplified using Immolase (BIOLINE, Tokyo, Japan) with primer sets as follows: *Tgfbi* Bis 1 F, 5'-GTTGTTTGTTTAGGATATTAATTGGG-3' and R, 5'-AAATACATCAACCCTACTAATACAC-3'; *Tgfbi* Bis 2 F, 5'-GAAATTGAAATTTGAGGATTAGTTTTT-3' and R, 5'-CCCTTATCTCATCAACCTCCA-3'; *Tgfbi* Bis 3 F, 5'-TTTTTTTTGATTTTAGGTAGAAGGG-3' and R, 5'-AAAATACCATACCAAACTCTTCATCA-3'. The PCR conditions were as follow: 95°C for 10 min, followed by 40 cycles of denaturation at 94°C for 30 sec, annealing at 58°C for 30 sec, and extension at 72°C for 1 min, and a final extension at 72°C for 10 min.

PCR products were digested with *Hha*I (Takara, Kyoto, Japan), *Acc*II (Takara) or *Hpy*Ch4IV (NEB, Ipswich, MA) at 37°C, or with *Taq*I (Takara) at 65 °C for 3 hr. Restricted fragments were assessed by agarose gel electrophoresis. Images were recorded and semiquantified using ImageJ software provided by National Institutes of Health (http://rsbweb.nih.gov/ij/). For electrophoresis using microchip electrophoresis system, band area for each fragment was quantified. Relative DNA methylation level of each genic region was calculated by the formula: DNA methylation status (%) = $100 \times I^C$ / ($I^{UC} + I^C$) where I^C and I^{UC} represent the intensities or areas of the digested and undigested bands, respectively.

For bisulfite sequencing, PCR products were cloned into pGEM T-Easy vector (Promega, Madison, USA), and 10 clones were sequenced for each sample.

RNA extraction and RT-PCR

Total RNA was extracted with TRIzol reagent (Invitrogen) according to the manufacturer's instructions. First strand cDNA was synthesized with SuperScript™ III First-Strand Synthesis System for RT-PCR (Invitrogen), and RT-PCR was performed using Taq DNA Polymerase (Promega) with primers as follows: *Tgfbi* F, 5'-ACCCTCACCTCCATGTACCA-3', R, 5'-TGCTGGATGTTGTTGGTGAT-3'; *β-actin* F, 5'-TTCTACAATGAGCTGCGTGTGG-3'; R, 5'-ATGGCTGGGGTGTTGAAGGT-3' and *Dnmt1* F, 5'-CAGGAGTGTGTGAGGGAG-3'; R, 5'-GGTGTCACTGTCCGACTTGC-3'. PCR conditions were as follow: 95°C for 1 min, followed by 30 cycles of denaturation at 94°C for 30 sec, annealing at 54°C for *Tgfbi*,

58°C for *β-actin* and 60°C for *Dnmt1* for 30 sec, and extension at 72°C for 1 min, and a final extension at 72°C for 5 min.

Chromatin immunoprecipitation (ChIP) assay

ChIP assays were performed as described previously (Hattori et al. 2004b) using a Chromatin Immunoprecipitation (ChIP) Assay Kit (Cat. No. 17-295; Upstate Biotechnology, Lake Placid, NY), with anti-acetylated histone H3 and H4 antibodies (Cat. No. 06-599 and 06-598; Upstate Biotechnology), anti-trimethylated H3K4 and H3K9 (Cat. No. ab8580 and ab8898; Abcam, Cambridge, UK), and anti-dimethylated H3K4, H3K9 and H3K27 (Cat. No. 07-030, 07-212 and 07-452; Upstate Biotechnology). Normal rabbit IgG (Cat. No. 12-370; Upstate Biotechnology) was used as a negative control to verify immunoprecipitation specificity. PCR was performed using primers as follows: Tgfbi Region 1 F, 5'-CTTAGCTTGGAGCCCTGATG-3'; R, 5'- AGGCACAGTATGGCACAGTATG-3'; Tgfbi Region 2 F, 5'-GCTTAGTAGTGGCGTGGTCTG-3'; R, 5'- CGGTGCTGGTGAAGTGAGAG-3'; and Tgfbi Region 3 F, 5'-AGATTGGGAAACCGAGTCCT-3'; R, 5'-GAGTGCGTCTCCGAAAACTT-3', with following PCR conditions: 95°C for 10 min, followed by 30 cycles of denaturation at 94°C for 30 sec, annealing at 62°C for Tgfbi Region 1, 58°C for Tgfbi Region 2, 54°C for Tgfbi Region 3 for 30 sec, and extension at 72°C for 1 min, and a final extension at 72°C for 10 min. Amount of each PCR product on an ethidium bromide stained gel-image was evaluated using ImageJ software.

RNA interference

Wild type ES cells and mutant ES cells deficient of *G9a* and *Suv39h1/Suv39h2* were transfected with siRNA duplexes (final concentration 20 nM, Dharmacon) using Lipofectamine 2000 (Invitrogen) according to the manufacturer's instructions. One additional round of transfection was performed under identical conditions 48 hr after the initial transfection. Cells were harvested 48 hr after the second transfection.

Protein extraction and Western blotting

Cells were lysed in RIPA buffer (50 mM Tris-HCl, pH8.0, 400 mM NaCl, 1% Nonident P-40, 1% sodium deoxycholate, 0.1% SDS, 1 mM phenylmethylsulfonyl fluoride, 5 μg/ml leupeptin, 1 μg/ml aprotinin, 5 μg/ml pepstatin and 0.5 mM EDTA). Cell lysate (10 μg) was subjected to SDS polyacrylamide gel electrophoresis on 15% gel, and were transferred onto membrane using iBlot® Dry Blotting System (Invitrogen). Transferred protein was probed with anti-GAPDH (1:2000 dilution; Imgenex, San Diego) and anti-H3K4me3 (1:500 dilution; Abcam), followed by 1:5000 diluted anti-mouse and anti-rabbit immunoglobulins conjugated with horseradish peroxidase (Wako Pure Chemicals). Protein was detected using Western Lightning ECL (Perkin Elmer, Waltham, MA).

Results

Gene Structure of *Tgfbi* Gene and CpG Distribution

Tgfbi has a CpG island spanning across upstream promoter region, transcription start site (TSS) and exon 1 (-162 to +93 in relative to TSS), with a CpG frequency of 69.5% and CpG_{obs}/CpG_{exp} of 0.78 (Fig. 2-1A). Region located downstream adjacent to the CpG island (+115~+370) is also relatively rich in CpG., and there were 38 CpGs in the CpG island and the adjacent CpG rich region. The upstream region flanking -805 to -632 is moderately rich in CpG, carrying 8 CpGs within a 173 bp fragment whereas downstream region from +519 to +937 contain relative low abundance of CpG, with and 7 CpGs within a length of 418 bp. In this chapter, we tentatively named the upstream region (-805~-632) as Region I, the CpG island and the adjacent CpG rich region (-162~+370) as Region II and the downstream region (+519~+937) as Region III.

In NIH/3T3 cells, Region I was almost fully methylated (Fig. 2-1B). All 8 CpGs scattering in the upstream region were heavily methylated. Similar to Region I, Region 3 was also fully methylated, with all 7 CpGs heavily methylated in its flanking region. Compared to Region I and III, Region II was less methylated. Almost all of the CpGs in the entire CpG island were approximately 70% methylated. At the adjacent CpG rich region, the 12 CpGs immediately following CpG island were also almost 70% methylated, whereas the 3 CpGs located 3' end of Region II were heavily methylated. Thus, *Tgfbi* genic regions in NIH/3T3 cells consist of a hypermethylated Region II flanking CpG island around TSS and the adjacent CpG rich region, surrounded by fully methylated Region I upstream and Region III downstream.

Effect of 5azadC on Methylation Pattern of *Tgfbi*

To address whether the hypermethylated regions are affected by 5azadC, cells were treated with 0.1 and 1 μM of 5azadC. At 0.1 μM, heavily methylated CpGs in Region I and Region III became moderately methylated (Fig. 2-1B). Region II was hypomethylated, and the methylation level was reduced to approximately 10% in both CpG island and the adjacent CpG rich region. These showed that 0.1 μM 5azadC could induce demethylation more than 50% in genic regions.

Interestingly, when we treated the cells with 1 μM 5azadC, all CpGs in Region I remained heavily methylated. The entire Region II was divided into two differentially methylated regions by 1 μM 5azadC: a fully demethylated CpG island and a hypermethylated CpG rich region consisted of 5 unmethylated CpGs and 10 heavily methylated CpGs. Region III was also less demethylated in 1 μM compared to 0.1 μM, with 2 out of 7 CpGs in the region were moderately demethylated. The results indicated that following 1 μM 5azadC treatment, *Tgfbi* genic regions was divided into highly susceptible CpG island and the demethylation resistant non-CpG island regions. These consistent with our previous study on T-DMRs and other genic regions that genic regions were resistant to 1 μM compared to 0.1 μM 5azadC.

Role of DNA methyltransferases on *Tgfbi*

As regions in *Tgfbi* were differentially demethylated by 5azadC, we wondered which Dnmt is responsible for methylation status of *Tgfbi*. We investigated the methylation status of *Tgfbi* in *Dnmt1* knock out and *Dnmt3a* and *3b* double knock out

ES cells. In wild type ES cells, the 4 CpGs located near TSS of Region I were moderately methylated, whereas the other 4 CpGs further from TSS were densely methylated (Fig. 2-2). The CpG island in Region II was almost totally unmethylated, and only a small portion of CpGs located downstream of the CpG rich region were methylated. Region III was hypermethylated in *Tgfbi*. There is a clear difference of the methylation pattern of Region II between ES cells and NIH/3T3 cells, indicating that the region is a unique T-DMR which involves the entire CpG island.

In *Dnmt1*$^{-/-}$ ES cells, Region II and Region III were almost completely unmethylated. The CpG rich region located downstream of Region II was also almost completely demethylated, whereas CpG island was fully demethylated. There was a slight methylation remained in *Tgfbi* following *Dnmt1* depletion. In *Dnmt3a*$^{-/-}$*3b*$^{-/-}$ ES cells, all regions in *Tgfbi* were totally unmethylated. These data indicated that CpG methylation is regulated by Dnmt1 as well as Dnmt 3a and 3b. In the absence of Dnmt1, Dnmt3a and 3b were responsible for methylation. In contrast, Dnmt1 was unable to methylate the genic regions when Dnmt3a and Dnmt3b were disrupted. Thus, treating the cells with 5azadC should mimic the intracellular preparation of *Dnmt1* knock out cells, as 5azadC is an inhibitor of Dnmt1.

Expression of *Tgfbi*

Tgfbi was expressed in NIH/3T3 cells. The expression increased when the cells were treated with 0.1 μM of 5azadC (Fig. 2-3A). In 1 μM 5azadC treated cells, the expression was also increased, despite having hypermethylated genic regions. To understand the mechanisms regulating *Tgfbi* expression, we investigated the status of

transcriptional active chromatin associated H3K4 methylation and histone acetylation in Region II, focusing on the CpG island region around the promoter and TSS (designated ChIP2) by ChIP analysis (Fig. 2-1A). The region covering 10 hypermethylated CpGs was highly enriched with H3K4me2 and H3K4me3 in NIH/3T3 cells (Fig. 2-3B). Following 0.1 μM 5azadC treatment, H3K4me2 remained the same level as untreated control, but H3K4me3 was slightly increased in the region. When cells were treated with 1 μM 5azadC, H3K4me2 was increased in the same region, whereas H3K4me3 had similar increment as those induced in 0.1 μM. Both H3K4 marks were elevated by 5azadC treatment, which concomitant with transcriptional increase. We confirmed the involvement of H3K4me3 in the transcriptional regulation of *Tgfbi* in NIH/3T3 cells by gene knockdown of *Wdr5*, one of the structural components in the yeast Set1 complex in H3K4 histone methyltransferases (Dou et al. 2006; Fig. 2-4).

We extended ChIP analysis to Region I and Region III. In NIH/3T3 cells, region covering the 4 CpGs at the 5' end of Region I (designated ChIP1) was also enriched with H3K4me2, and the level was concentration dependently increased by 5azadC. H3K4me3 was less enriched than H3K4me2 in the same region, and the mark was also increased by 5azadC. In Region III, region flanking the 5 CpGs at the 3' end (designated ChIP3) had high abundance of H3K4me2 and H3K4me3. Similar to those in ChIP1 and ChIP2 regions, the H3K4 marks were also increased by 5azadC. These showed that increment of H3K4 following 5azadC treatment occurred in all genic regions in *Tgfbi* regardless CpG abundance.

Tgfbi gene regions were highly enriched with histone H3 acetylation mark (AcH3)

in NIH/3T3 cells. The level of AcH3 in ChIP2 region was comparatively higher than those in ChIP1 and ChIP3 regions. Meantime, histone H4 acetylation (AcH4) was low in ChIP1, and its level was even lower in ChIP2 and ChIP3. At 0.1 μM 5azadC, both acetylation marks were largely increased at the ChIP1, and were slightly increased in ChIP2 and ChIP3.

Surprisingly, following 1 μM 5azadC treatment, AcH3 level decreased in ChIP2 compared to untreated ones, although all CpGs in this region were totally umethylated. Likewise, decrement of AcH3 was also observed in ChIP1 which contained all heavily methylated CpGs and also in ChIP3 which was partially methylated. In contrast to AcH3, AcH4 levels remained almost unaltered in all 3 regions at the same concentration. These showed that 1 μM 5azadC caused AcH3 decrease in genic regions, and the decrease is irrelevant to DNA methylation status of the genic regions. Reduction of the mark was also in contradictory to transcriptional increase induced by the concentration.

To address whether similar histone modification changes occurred following Dnmt knock out, ChIP analysis was also performed on the same regions in Dnmt deficient ES cells. In ES cells, all regions were enriched with both H3K4 marks (Fig. 2-5B). When Dnmt1 was depleted, H3K4me2 increased in all regions, with higher fold increased in ChIP1 and ChIP3. Increment of H3K4me3 was also occurred in all regions, showing identical results as observed in 5azadC treated cells. Concurrently, *Tgfbi* expression increased in *Dnmt1$^{-/-}$* ES cells (Fig. 2-5A). In *Dnmt3a$^{-/-}$3b$^{-/-}$* ES cells, H3K4me2 was minimally altered in ChIP1 and ChIP2 regions. The mark was increased in ChIP3, but in a lesser extent compared to those induced in *Dnmt1$^{-/-}$*. H3K4me3 marks were also

slightly increased in all regions. Limited increment of both H3K4 marks in *Dnmt3a^{-/-}3b^{-/-}* corresponded to a only slight increase in the expression.

ChIP2 region had high abundance of AcH3 in ES cells. Comparatively, ChIP1 and ChIP3 had relatively low level of the same mark. Following disruption of Dnmts, the acetylation mark was reduced in all regions. Reduction of AcH3 mark was more severe in *Dnmt3a^{-/-}3b^{-/-}* compared to those in *Dnmt1^{-/-}*. On the other hand, AcH4 was less enriched in ChIP1 region, and its abundance was even lower in ChIP2 and ChIP3 in ES cells. A drastic reduction of the mark was observed in ChIP1 in Dnmt knock out cells, whereas slight reduction occurred in ChIP2 and ChIP3. Taken together, the acetylation mark, especially AcH3, was reduced following Dnmt inhibition or disruption.

Resistance of *Tgfbi* to 5azadC Induced Demethylation

To gain insight into the mechanism of resistance to demethylation induced by 5azadC, we investigated the heterochromatic associated histone marks focusing on the highly resistant Region I and Region III and the demethylation sensitive Region II. Using antibodies against H3K9me2, H3K9me3 and H3K27me2, ChIP assays were performed on ChIP1, ChIP2 and ChIP3 regions.

H3K9me2 level was low in upstream region ChIP1 in NIH/3T3 cells (Fig. 2-3B). The level was lower at ChIP2 compared to the level in ChIP1, and was more reduced in ChIP3. On the other hand, H3K9me3 was minimal at ChIP2, and the level was diminished in both ChIP1 and ChIP3. Following 5azadC treatment, H3K9me2 levels at the regions were reduced, with slightly more reduction at 1 μM. Interestingly,

degradation of H3K9me2 was accompanied by increment of H3K9me3. At ChIP2, H3K9me3 was increased at 0.1 μM 5azadC, and was further increased at 1 μM. H3K9me3 was also increased at almost the same extent in ChIP1 at both concentrations. At ChIP3, the increment occurred concentration dependently. These showed that 5azadC induced demethylation might lead to the decrease of di-methylation, followed by the increase of tri-methylation of the H3K9 marks at all *Tgfbi* regions. Changes in the H3K9 marks were more intense in 1 μM compared to 0.1 μM. H3K27me2 was evenly enriched the regions in NIH/3T3 cells, and was minimally altered by 5azadC treatment.

In ES cells, ChIP2 flanking the CpG island barely contained both H3K9 marks, the marks were at minimal levels at the CpG island and TSS region (Fig. 2-5B). Concurrently, ChIP 1 and ChIP had higher level of both H3K9 marks compared to ChIP2, but the enrichments were relatively low compared to H3K4 and acetylation marks. In *Dnmt3a$^{-/-}$3b$^{-/-}$* ES cells, H3K9me2 increased in all regions, which were completely unmethylated. In adverse, H3K9me3 decreased severely at all regions, and the mark was depleted at ChIP2 region.

Following *Dnmt1* knocked out, H3K9me2 was lightly reduced in ChIP1 and ChIP3, and was diminished in ChIP2. In contrast, H3K9me3 was maintained at almost the same level as those in wild type, which coincided with a small level of DNA methylation observed at all of the regions in *Dnmt1$^{-/-}$* ES cells. All together, the results were in parallel with those in 5azadC induced combination, and were in contrary to those in Dnmt3a and 3b knock out cells, implying that increasing level of H3K9me3 was

associated with maintenance of DNA methylation in the genic regions.

Role of H3K9 methyltransferase in *Tgfbi*

Increase of H3K9me3 in genic regions following 5azadC treatment suggested the involvement of H3K9 methyltransferase in the resistant mechanism. To address which enzyme is responsible for the histone methylation following Dnmt1 disturbance, we transfected H3K9 methyltransferase *Suv39h1* and *Suv39h2* double knock out ES cells and *G9a* knock out ES cells with siRNA targeting on Dnmt1, and investigated DNA methylation status in *Tgfbi* regions with bisulfite sequencing.

In wild type ES cells used for *Suv39h* knock out, the CpGs in Region I had a methylation level of 81.3% (Fig. 2-6B). The CpG island of Region II was almost completely demethylated, whereas the 7 CpG located at the 3' end of Region II was partially methylated. Region III had a methylation level of 78.6%. Overall methylation level of these regions was higher than those observed in the J1 line wild type ES cells used for *Dnmt* knock out, due to strain and genomic differences. In *Suv39h* deficient ES cells, methylation levels of Region I, II and III were similar to those observed in wild type, indicating that Suv39h methyltransferases do not intervene in DNA methylation in genic regions.

Following *Dnmt1* knocked down, CpG methylation levels in both wild type and mutant cells of each region were reduced. Interestingly, although Dnmt1 expression was reduced to 60% of the regular level (Fig. 2-6A), DNA methylation levels in Region I and III were differentially reduced in wild type and in mutant cells after *Dnmt1* knocked

down. The methylation levels of Region I and III in mutant cells after *Dnmt1* knocked down were relatively 30-40% higher than the methylation levels in wild type cells in similar conditions. DNA methylation levels in Region II were almost similar in wild type and mutant cells after *Dnmt1* knock down. These showed that a demethylation resistance was induced in non-CpG island genic regions corresponding to *Dnmt1* knock down in *Suv39h$^{-/-}$* ES cells.

We next investigated the CpG methylation status in *Tgfbi* regions following *Dnmt1* knocked down in *G9a* deficient ES cells and the wild type strain (Fig. 2-7A). In the wild type ES cells, Region I had a methylation level of 40% (Fig. 2-7B). Region II was almost completely unmethylated, having a methylation level of 4%, whereas Region III was partially methylated with a methylation level of 58.9%. Intriguingly, CpG methylation level in each region decreased following G9a disruption. In *G9a$^{-/-}$* ES cells, the CpG methylation level in Region I was about 10.9%, which was almost 30% lower than the level in wild type. Region II in *G9a* deficient cells was also unmethylated, whereas the CpG methylation level in Region III was 20% lower than the level observed in wild type. The data was in contrary to those observed in Suv39h methyltransferases, and indicated that G9a contribute to DNA methylation level in *Tgfbi*.

Following Dnmt1 knock down, the CpG methylation level in Region I was reduced to around 20% in wild type ES cells. In *G9a* disrupted cells, the methylation level was reduced from 10% to 6%. DNA demethylation in Region III was also more severe in *G9a$^{-/-}$* ES cells compared to wild type when Dnmt1 was knocked down. Region II was

almost completely demethylated when Dnmt1 was disturbed, as the region was originally hypomethylated in both kinds of cells. Thus, in contrast to *Suv39h* deficient ES cells, demethylation adherent to *Dnmt1* knock down in *Tgfbi* regions in *G9a* deficient ES cells was vigorous than those in wild type ES cells. Resistance to demethylation observed in *Suv39h* deficient ES cells in *Tgfbi* regions was not observed in *G9a* deficient cells, indicating that G9a was involved in the resistance mechanisms.

Discussion

Using chemical inhibitory of Dnmt, Dnmt knock out and knock down approaches, current studies reveal the complex epigenetic mechanisms involved in regulation of *Tgfbi* and how 5azadC affects the epigenetic modifications. When Dnmt is inhibited by 5azadC, DNA demethylation occurs and together with H3K4 increment, gene expression increased. However, 5azadC treatment is also accompanied by increasing of repressive mark H3K9me3, which is not observed in *Dnmt1*$^{-/-}$ cells. H3K9me3 level increased with 5azadC concentrations, concurrently leads to demethylating resistance. In addition, histone methyltransferase G9a is involved in DNA methylation maintenance in *Tgfbi*, which might perhaps mediate H3K9 trimethylation. Thus, mechanism actions of 5azadC in reversing silenced genes are not just simple as DNA demethylation as previously thought.

A large decrement of DNA methylation in gene region and retroelements reflects the involvement of G9a in regulation of DNA methylation (Ikegami et al. 2007; Dong et al. 2008; Tachibana et al. 2008). However, it is still a doubt whether G9a mediates recruitment of Dnmts to targeted regions or it directly methylates DNA. Although it has been reported that human G9A interacts with DNMT1 (Esteve et al. 2006), Dnmt3a and 3b had shown to induce de novo methylation on *Mage-2* and *Wfdc15a* in mouse ES cells, which are also the target regions of G9a/GLP complex (Tachibana et al. 2008). As Dnmt1, Dnmt3a and Dnmt3b shares the same target regions, Dnmt3a and 3b might maintain DNA methylation in gene regions when Dnmt1 is disrupted. However, Dnmt1 could not regulate DNA methylation in gene regions in *Dnmt3a*$^{-/-}$*3b*$^{-/-}$ cells, due to preference of Dnmt1 to the non-coding repetitive sequences, whereas Dnmt3a and 3b

favors coding gene regions (Chapter 1, Hattori et al. 2004b). G9a might be responsible to recruit Dnmt3a and 3b to methylate genic regions when Dnmt1 is disturbed, but does not recruit Dnmt1 when Dnmt3a and 3b is disrupted, thereby results in complete demethylation.

Involvement of G9a, but not Suv39h in DNA methylation maintenance of *Tgfbi* had raised questions on the substrate specificity of the histone methyltransferases. *G9a* depletion caused dramatic decrease in H3K9me1 and H3K9me2 in the euchromatin of ES cells, whereas ES cells with disrupted *Suv39h1* and *Suv39h2* leads to drastic reduction in H3K9me3 in the pericentromeric regions (Tachibana et al. 2002, 2005; Lehnertz et al. 2003; Martens et al. 2005). As current results showed that H3K9me2 was decreased and H3K9me3 was increased in 5azadC treated cells, the role played by G9a still need to be elucidated. Suv39h did not contribute to DNA methylation, probably due to its functional preference on the heterochromatin regions (Lehnertz et al. 2003; Martens et al. 2005). There is a possibility that 5azadC affects G9a methyltransferase itself, reducing H3K9me2 and H3K27me2 levels and causing DNA methylation. If this is the case, increase of H3K9me3 might involve other H3K9 methyltransferases such Eset, GLP, CLL8 (Kouzarides, 2007).

Recent studies show that *Tgfbi* is also associated with cancer development, and it is epigenetically inactivated in various cancer cell lines (Shao et al. 2006; Shah et al. 2008). Existence of T-DMR in *Tgfbi* in our studies provides evidence that the T-DMR might contribute to the gene functions. Aberrant methylation in the T-DMR which covers the CpG island at the promoter region and transcription start site might caused

abnormalities and dysfunctions that involves the gene functioning such as cancers and corneal dystrophies. *Tgfbi* expression is induced by both demethylation and increase of H3K4 methylation. The ability of 5azadC to induce demethylation at the T-DMR followed by transcriptional increase provides a treatment option for the abnormalities. Nonetheless, appropriate concentrations should be used due to its strong effect on non-genic regions.

Figure 2-1

A
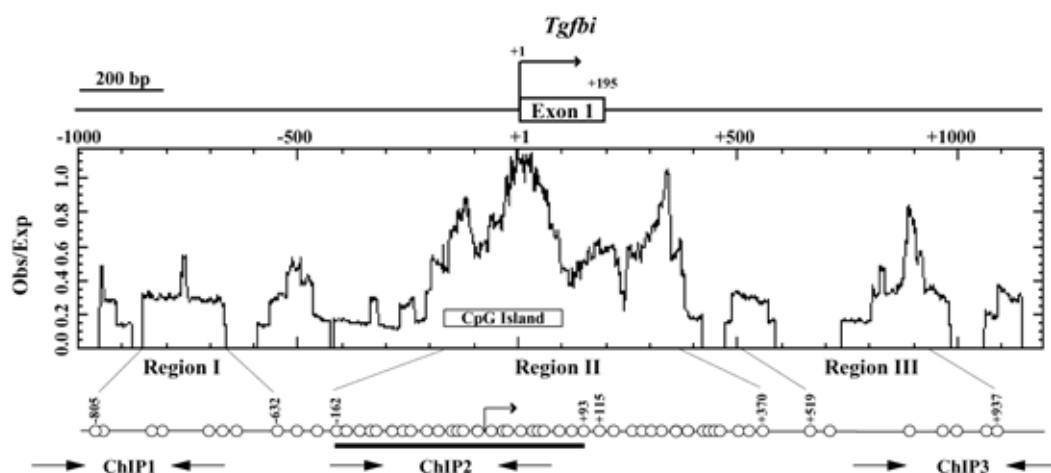
B
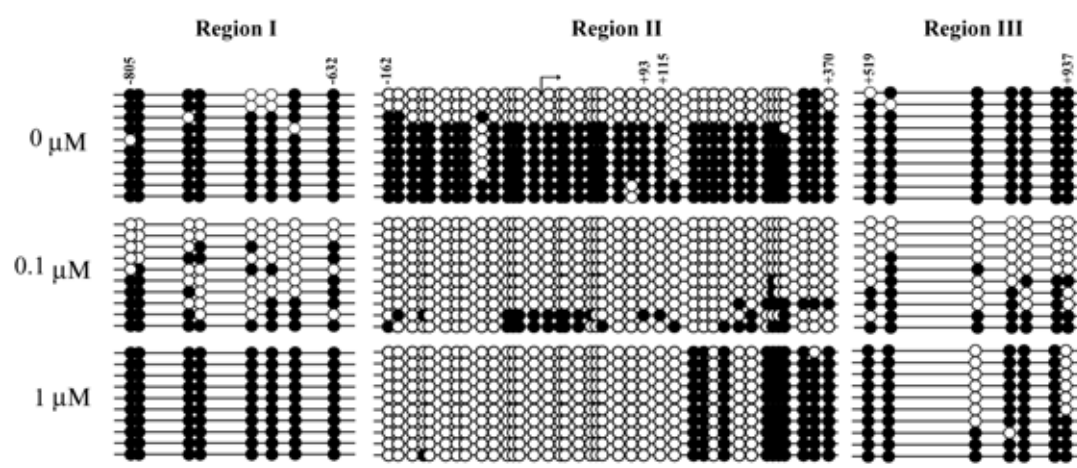
Figure 2-1. DNA methylation status of Tgfbi gene .

A, **Schematic diagram of the gene structure of Tgfbi gene.** Upper panel shows the gene structure of Tgfbi gene, in parallel with the CpG distribution shown in the middle panel. Middle panel demonstrate the CpG frequency of Tgfbi gene (-1000 bp to +1200 bp in relative to transcription start site) and the location of CpG island. Lower panel shows the positions of CpG sites in Region I (-805 bp to -632 bp), Region II (-162 bp to +370 bp), Region III (+519 bp to +937 bp) analyzed by bisulfite sequencing. Circles and numbers indicate positions of CpGs relative to transcription start site (+1). Arrows in the bottom panel indicate the primer positions for ChIP assay. Black bar indicates CpGs which are flanked in CpG island.

B, **DNA methylation status of Tgfbi gene in NIH/3T3 cells before and after treating with 5azadC analyzed by bistulfite sequencing.** Methylation status is depicted by open (unmethylated) and closed (methylated) circles for each CpG site. Numbers indicate positions of CpGs relative to transcription start site (+1). Black bar indicates CpGs which are flanked in CpG island.

Figure 2-2
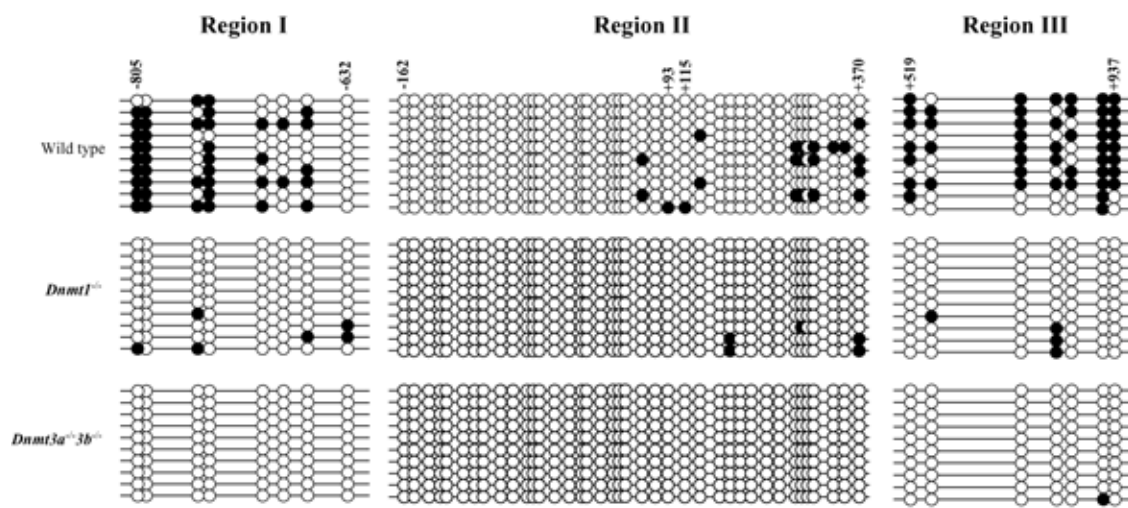
Figure 2-2. DNA methylation status of Tgfbi gene in Dnmt knock out ES cells.

DNA methylation status of Tgfbi gene in wild type, *Dnmt1$^{-/-}$* and *Dnmt3a$^{-/-}$3b$^{-/-}$* ES cells analyzed by bisulfite sequencing.

Figure 2-3

A

B

C
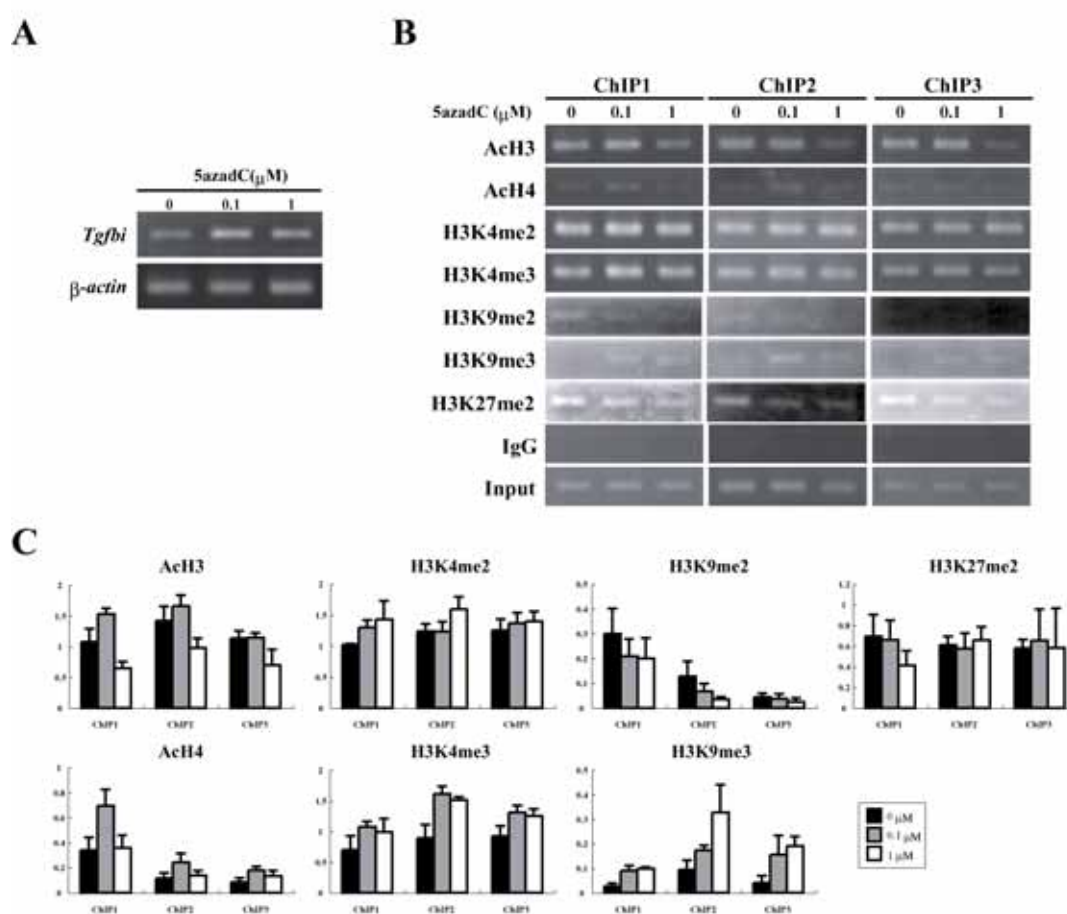
Figure 2-3. Effect of 5azadC on Tgfbi gene expression and histone modification status.

A, **Expression of *Tgfbi* at 0, 0.1 and 1 μM 5azadC analyzed by RT-PCR.** Expression level of β-actin was used as the internal control.

B& C, **Histone modification analysis of 0, 0.1 and 1 μM 5azadC treated samples by ChIP.** Analyzed regions are indicated by arrowed "ChIP" in the schematic diagram in Fig. 2-1A. DNA immunoprecipitated with respective antibodies was amplified by PCR and electrophoresed. Relative intensities of PCR bands to those of the input DNA, represented by the means ± S.E. of 3 independent PCRs of 3 cultures are shown in panel C.

Figure 2-4

A
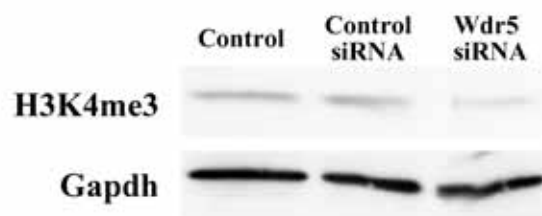
B
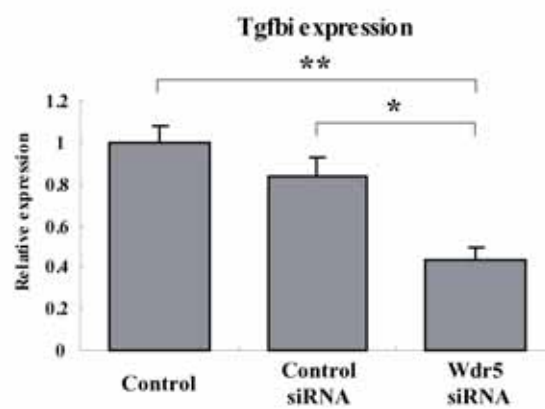
Figure 2-4. Effect of H3K4me3 on *Tgfbi* expression.

A, **Protein levels of H3K4me3 in mock and *Wdr5* knocked down NIH/3T3 cells.** *Gapdh* levels were used as loading control.

B, **Expression level of Tgfbi in mock and Wdr5 knocked down NIH/3T3 cells.**

Figure 2-5

A

ES

	WT	*Dnmt1⁻/⁻*	*Dnmt3a⁻/⁻3b⁻/⁻*
Tgfbi			
β-actin			

B

C
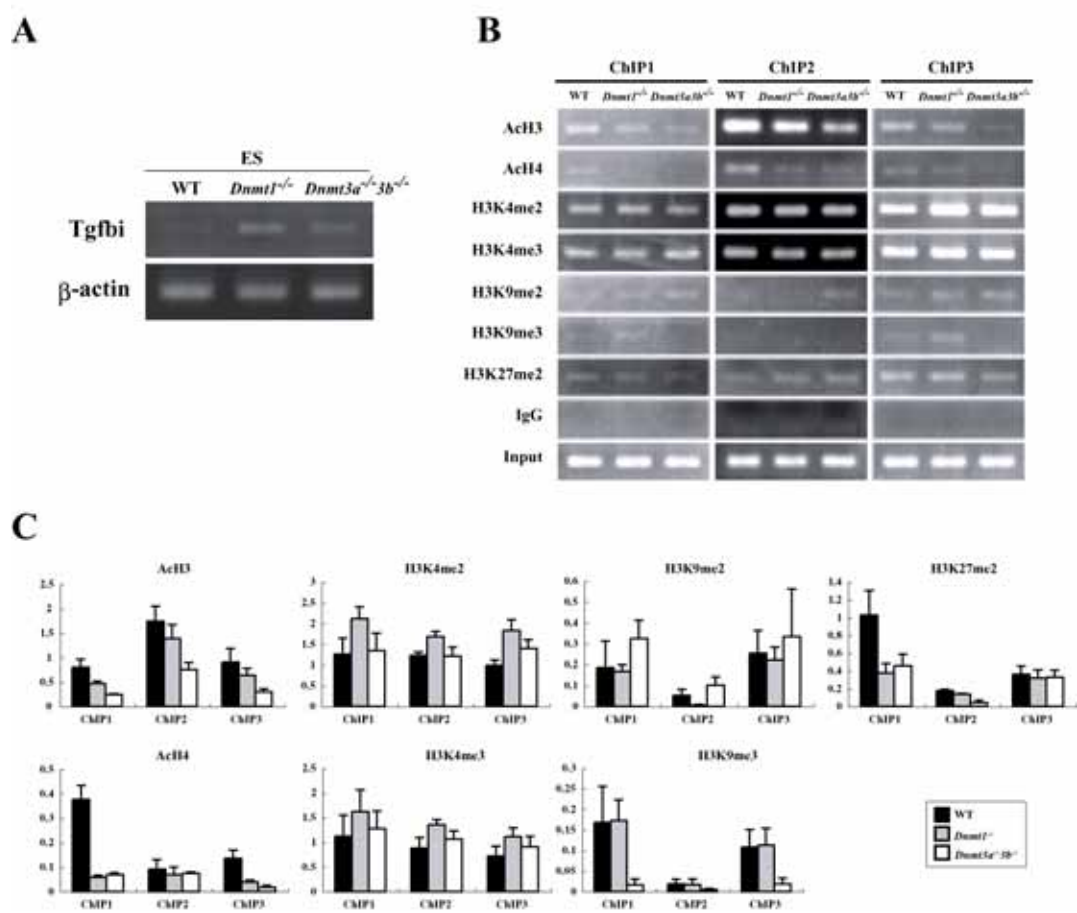
Figure 2-5. Histone modification patterns of Tgfbi in ES cells deficient of *Dnmt1*, *Dnmt3a* and *Dnmt3b*.

A, **Expression of *Tgfbi* in *Dnmt1$^{-/-}$*, *Dnmt3a$^{-/-}$3b$^{-/-}$* ES cells analyzed by RT-PCR.** Expression level of β-actin was used as the internal control.

B& C, **Histone modification analysis of ChIP1, ChIP2 and ChIP3 regions in Dnmt deficient ES cells.** Analyzed regions are indicated by arrowed "ChIP" in the schematic diagram in Fig. 2-1A. DNA immunoprecipitated with respective antibodies was amplified by PCR and electrophoresed. Relative intensities of PCR bands to those of the input DNA, represented by the means ± S.E. of 3 independent PCRs of 2 cultures are shown in panel C

Figure 2-6

A

Dnmt1 expression

B

WT

Control

81.3 %

Dnmt1 siRNA

25.0 %

1.0 %

2.6 %

40.9 %

17.0 %

Suv39h⁻/⁻

Control

87.5 %

Dnmt1 siRNA

60.9 %

2.1 %

2.6 %

50.6 %

23.9 %

Region I   Region II   Region III
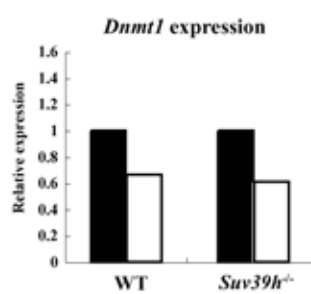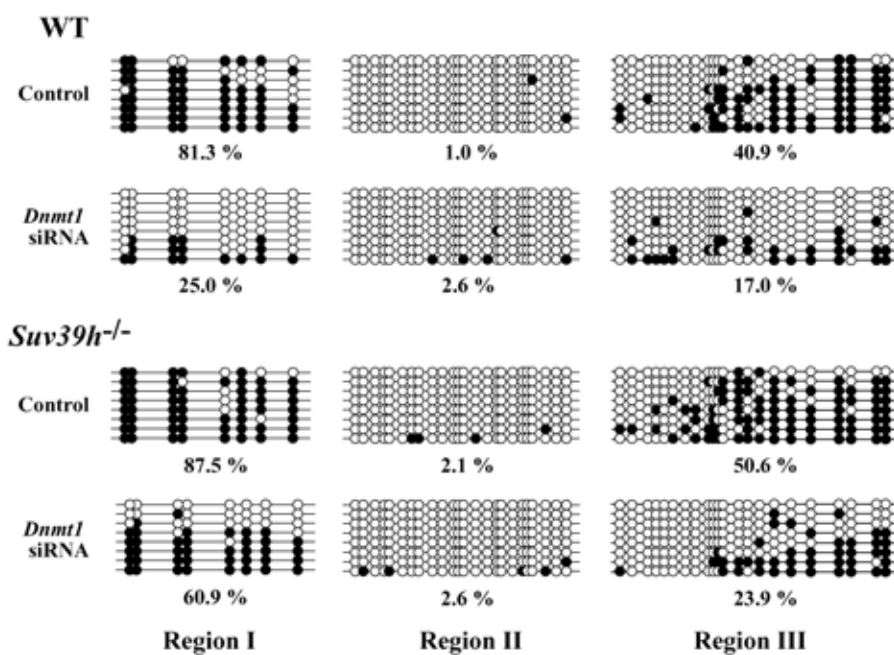
Figure 2-6. Effect of Dnmt1 knock down in *Suv39h* deficient cells.

A, **Dnmt1 knock down efficiency evaluated by real time RT-PCR.** Relative expression levels are normalized to β-actin expression level of respective samples.

B, **DNA methylation analysis on Tgfbi in *Suv39h* deficient cells transfected with siRNA targeting Dnmt1, by bisulfite sequencing.** DNA methylation levels of each region, represented by percentage of methylation, were indicated.

Figure 2-7

A
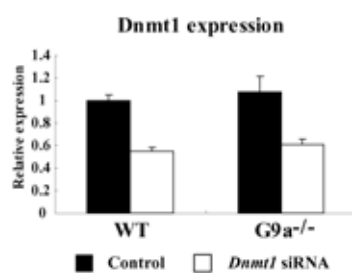
B
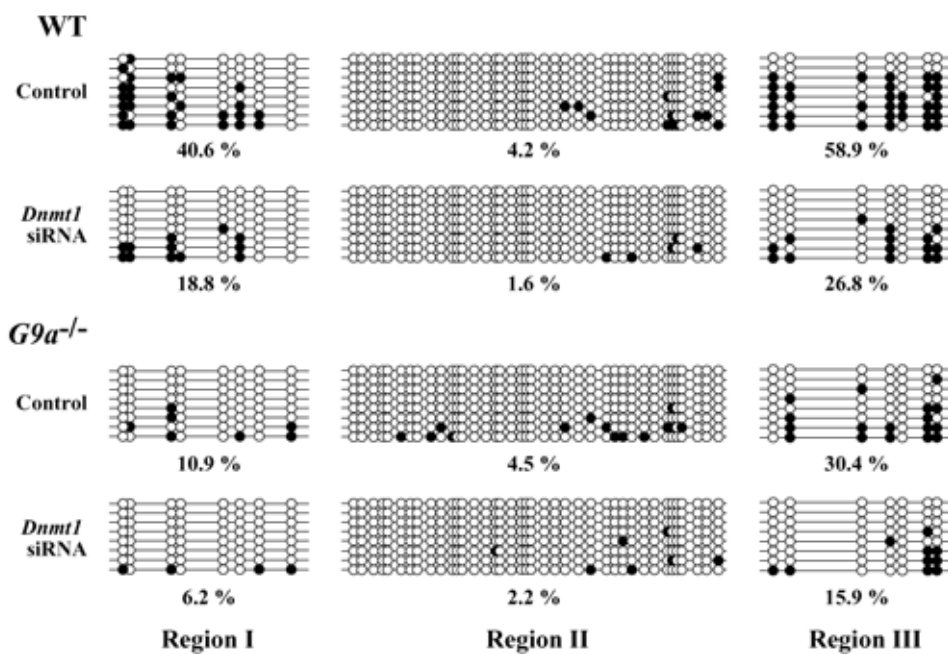
Figure 2-7. Effect of Dnmt1 knock down in *G9a* deficient cells.

A, **Dnmt1 knock down efficiency evaluated by real time RT-PCR.** Relative expression levels are normalized to β-actin expression level of respective samples.

B, **DNA methylation analysis on Tgfbi in *G9a* deficient cells transfected with siRNA targeting Dnmt1, by bisulfite sequencing.** DNA methylation levels of each region, represented by percentage of methylation, were indicated.

GENERAL DISCUSSION

General Discussion

Understanding the mechanisms underlying epigenetic disorders allows more treatment options for recovery. However, considering dynamic changes and diverse interactions in between DNA methylation and histone modifications, detailed evaluation is needed before the epigenetic drugs are clinically used. This thesis shows how 5-aza-2'-deoxycytidine or decitabine, a clinically approved drug for myelodysplastic syndrome, induced distinct effect on the non-genic repetitive sequences and genic regions.

In Chapter 1, I showed that 5azadC affects both genic regions and non-targeted repetitive sequences. Its demethylating effect on genic regions is restricted on certain effective concentrations. Increasing treatment dosage might not be effective to induce demethylation in targeted gene regions, but will lead to genome-wide hypomethylation which is associated with genomic instability and cancer (Almeida et al. 1993; Ehrlich 2002; Rodriguez et al. 2006). Hypomethylation of the repetitive sequences has been reported to be associated with chronic myeloid leukemia deterioration (Roman-Gomez et al. 2005; 2008). At the same time, 5azadC treatment was accompanied by unique combination of histone modifications, including increasing level of the heterochromatic H3K9me3 mark and decreasing level of euchromatin associated AcH3. Such combination changes might contribute to the demethylating resistance observed in genic regions.

In Chapter 2, I studied how DNA methylation and post-translational histone

modifications play central roles in regulating a disease causing gene. *Tgfbi*, a gene that is associated with cornea development and tumor suppressing, has been found to be epigenetically regulated, besides causing cornea dystrophies by mutations. Maintenance of DNA methylation pattern in *Tgfbi* involved DNA methyltransferase and histone methyltransferase G9a. Expression of *Tgfbi* is perhaps influenced by DNA hypomethylation and H3K4 levels, as increment of these marks was accompanied by gene upregulation following Dnmt inhibition (Fig. GD-1). Such assumption provides explanation on how 5azadC alone can induce re-expression of certain silenced genes that do not have apparent CpG island hypermethylation (Soengas et al. 2001; Zhu et al. 2001). Although 5azadC binds directly to DNA methyltransferase, but it might also indirectly affects other enzymes such as G9a in its mechanism of action, causing H3K9me3 elevation that contribute to demethylating-resistance. It is important to minimize the disturbance of the epigenetic balance when using an epigenetic drug for treatment.

It is of interest that resistance of genic regions to 5azadC involved H3K9 methyltransferase and Dnmts. A proposed model for the resistance mechanisms in genic regions is shown in Fig. GD-2. 5azadC inhibits Dnmt1 and causes strong demethylation hypermethylated repetitive sequences and genic regions. Due to cellular response to perhaps global hypomethylation or stress environment, H3K9me3 level in genic regions was increased, mediated by G9a histone methyltransferase. As Dnmt1, Dnmt3a and Dnmt3b share target gene regions, H3K9me3 increment induced recruitment of Dnmt3a and Dnmt3b to target regions and cause re-methylation.

Current findings are important for development of 5azadC for clinical use. Its strong effect on repetitive sequences when overdosed, involvement of other epigenetic factors in its mechanism actions should be taken in account to ensure its efficiency and safety in disease treatment.
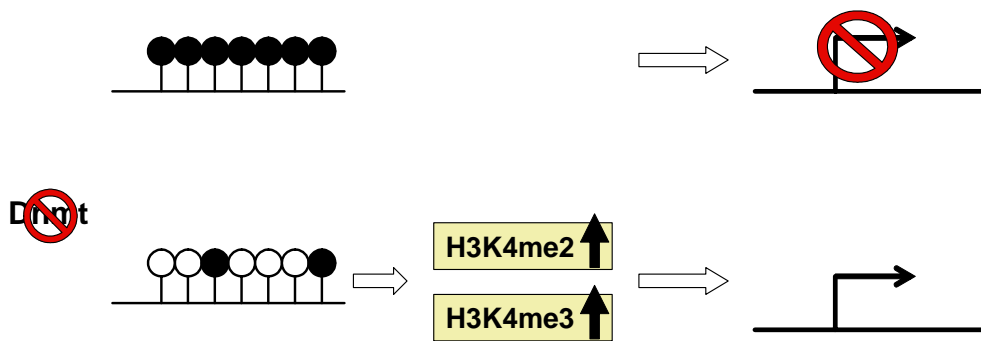
Figure GD-1. Mechanisms of gene activation by Dnmt inhibition.
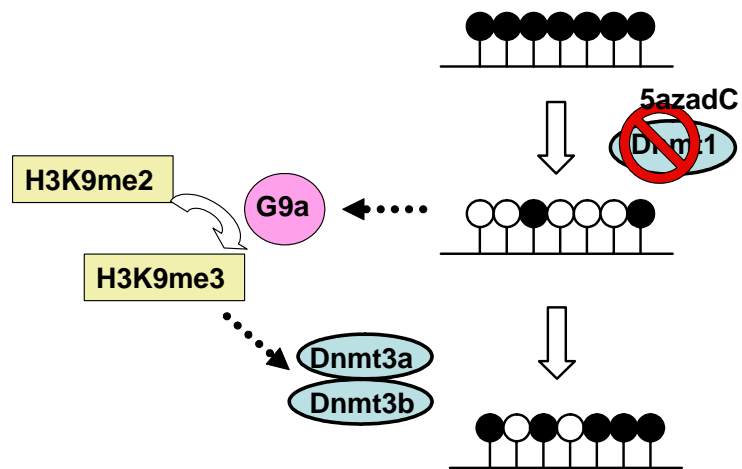
Figure GD-2. Model of resistance of genic regions to 5azadC.

References

Almeida, A., Kokalj-Vokac, N., Lefrancois, D., Viegas-Pequignot, E., Jeanpierre, M., Dutrillaux, B., and Malfoy, B. (1993). Hypomethylation of classical satellite DNA and chromosome instability in lymphoblastoid cell lines. Hum Genet 91, 538-546
.

Bustamante, M., Tasinato, A., Maurer, F., Elkochairi, I., Lepore, M.G., Arsenijevic, Y., Pedrazzini, T., Munier, F.L., and Schorderet, D.F. (2008). Overexpression of a mutant form of TGFBI/BIGH3 induces retinal degeneration in transgenic mice. Mol Vis 14, 1129-1137.

Chen, R.Z., Pettersson, U., Beard, C., Jackson-Grusby, L., and Jaenisch, R. (1998). DNA hypomethylation leads to elevated mutation rates. Nature 395, 89-93.

Chen, T., Ueda, Y., Dodge, J.E., Wang, Z., and Li, E. (2003). Establishment and maintenance of genomic methylation patterns in mouse embryonic stem cells by Dnmt3a and Dnmt3b. Mol Cell Biol 23, 5594-5605.

Cheng, J.C., Weisenberger, D.J., Gonzales, F.A., Liang, G., Xu, G.L., Hu, Y.G., Marquez, V.E., and Jones, P.A. (2004). Continuous zebularine treatment effectively sustains demethylation in human bladder cancer cells. Mol Cell Biol 24, 1270-1278.

Cortez, C.C., and Jones, P.A. (2008). Chromatin, cancer and drug therapies. Mutat Res.

Creusot, F., Acs, G., and Christman, J.K. (1982). Inhibition of DNA methyltransferase and induction of Friend erythroleukemia cell differentiation by 5-azacytidine and 5-aza-2'-deoxycytidine. J Biol Chem 257, 2041-2048.

Daskalakis, M., Nguyen, T.T., Nguyen, C., Guldberg, P., Kohler, G., Wijermans, P., Jones, P.A., and Lubbert, M. (2002). Demethylation of a hypermethylated P15/INK4B gene in patients with myelodysplastic syndrome by 5-Aza-2'-deoxycytidine (decitabine) treatment. Blood 100, 2957-2964.

Davidson, S., Crowther, P., Radley, J., and Woodcock, D. (1992). Cytotoxicity of 5-aza-2'-deoxycytidine in a mammalian cell system. Eur J Cancer 28, 362-368.

de Lima, M., Ravandi, F., Shahjahan, M., Andersson, B., Couriel, D., Donato, M., Khouri, I.,

Gajewski, J., van Besien, K., Champlin, R., et al. (2003). Long-term follow-up of a phase I study of high-dose decitabine, busulfan, and cyclophosphamide plus allogeneic transplantation for the treatment of patients with leukemias. Cancer 97, 1242-1247.

Dong, K.B., Maksakova, I.A., Mohn, F., Leung, D., Appanah, R., Lee, S., Yang, H.W., Lam, L.L., Mager, D.L., Schubeler, D., et al. (2008). DNA methylation in ES cells requires the lysine methyltransferase G9a but not its catalytic activity. EMBO J 27, 2691-2701.

Dou, Y., Milne, T.A., Ruthenburg, A.J., Lee, S., Lee, J.W., Verdine, G.L., Allis, C.D., Roeder, R.G., et al. (2006). Regulation of Mll1 H3K4 methyltransferase activity by its core components. Nat Struct Mol Biol 13, 713-719.

Ehrlich, M. (2002). DNA methylation in cancer: too much, but also too little. Oncogene 21, 5400-5413.

Esteller, M., Hamilton, S.R., Burger, P.C., Baylin, S.B., and Herman, J.G. (1999). Inactivation of the DNA repair gene O6-methylguanine-DNA methyltransferase by promoter hypermethylation is a common event in primary human neoplasia. Cancer Res 59, 793-797.

Fahrner, J.A., Eguchi, S., Herman, J.G., and Baylin, S.B. (2002). Dependence of histone modifications and gene expression on DNA hypermethylation in cancer. Cancer Res 62, 7213-7218.

Freitag, M., and Selker, E.U. (2005). Controlling DNA methylation: many roads to one modification. Curr Opin Genet Dev 15, 191-199.

Fuks, F., Hurd, P.J., Wolf, D., Nan, X., Bird, A.P., and Kouzarides, T. (2003). The methyl-CpG-binding protein MeCP2 links DNA methylation to histone methylation. J Biol Chem 278, 4035-4040.

Hackanson, B., Robbel, C., Wijermans, P., and Lubbert, M. (2005). In vivo effects of decitabine in myelodysplasia and acute myeloid leukemia: review of cytogenetic and molecular studies. Ann Hematol 84 Suppl 1, 32-38.

Hattori, N., Abe, T., Hattori, N., Suzuki, M., Matsuyama, T., Yoshida, S., Li, E., and Shiota, K. (2004a). Preference of DNA methyltransferases for CpG islands in mouse embryonic stem cells.

Genome Res 14, 1733-1740.

Hattori, N., Nishino, K., Ko, Y.G., Hattori, N., Ohgane, J., Tanaka, S., and Shiota, K. (2004b). Epigenetic control of mouse Oct-4 gene expression in embryonic stem cells and trophoblast stem cells. J Biol Chem 279, 17063-17069.

Herman, J.G., Umar, A., Polyak, K., Graff, J.R., Ahuja, N., Issa, J.P., Markowitz, S., Willson, J.K., Hamilton, S.R., Kinzler, K.W., et al. (1998). Incidence and functional consequences of hMLH1 promoter hypermethylation in colorectal carcinoma. Proc Natl Acad Sci U S A 95, 6870-6875.

Ikegami, K., Iwatani, M., Suzuki, M., Tachibana, M., Shinkai, Y., Tanaka, S., Greally, J.M., Yagi, S., Hattori, N., and Shiota, K. (2007). Genome-wide and locus-specific DNA hypomethylation in G9a deficient mouse embryonic stem cells. Genes Cells 12, 1-11.

Issa, J.P., Garcia-Manero, G., Giles, F.J., Mannari, R., Thomas, D., Faderl, S., Bayar, E., Lyons, J., Rosenfeld, C.S., Cortes, J., et al. (2004). Phase 1 study of low-dose prolonged exposure schedules of the hypomethylating agent 5-aza-2'-deoxycytidine (decitabine) in hematopoietic malignancies. Blood 103, 1635-1640.

Jabbour, E., Issa, J.P., Garcia-Manero, G., and Kantarjian, H. (2008). Evolution of decitabine development: accomplishments, ongoing investigations, and future strategies. Cancer.

Jackson, J.P., Lindroth, A.M., Cao, X., and Jacobsen, S.E. (2002). Control of CpNpG DNA methylation by the KRYPTONITE histone H3 methyltransferase. Nature 416, 556-560.

Jeong, K.S., and Lee, S. (2005). Estimating the total mouse DNA methylation according to the B1 repetitive elements. Biochem Biophys Res Commun 335, 1211-1216.

Ji, W., Hernandez, R., Zhang, X.Y., Qu, G.Z., Frady, A., Varela, M., and Ehrlich, M. (1997). DNA demethylation and pericentromeric rearrangements of chromosome 1. Mutat Res 379, 33-41.

Jones, P.L., Veenstra, G.J., Wade, P.A., Vermaak, D., Kass, S.U., Landsberger, N., Strouboulis, J., and Wolffe, A.P. (1998). Methylated DNA and MeCP2 recruit histone deacetylase to repress transcription. Nat Genet 19, 187-191.

Joseph, A., Mitchell, A.R., and Miller, O.J. (1989). The organization of the mouse satellite DNA at

centromeres. Exp Cell Res 183, 494-500.

Juttermann, R., Li, E., and Jaenisch, R. (1994). Toxicity of 5-aza-2'-deoxycytidine to mammalian cells is mediated primarily by covalent trapping of DNA methyltransferase rather than DNA demethylation. Proc Natl Acad Sci U S A 91, 11797-11801.

Kouzarides, T. (2007). Chromatin modifications and their function. Cell 128, 693-705.

Lachner, M., and Jenuwein, T. (2002). The many faces of histone lysine methylation. Curr Opin Cell Biol 14, 286-298.

Lehnertz, B., Ueda, Y., Derijck, A.A., Braunschweig, U., Perez-Burgos, L., Kubicek, S., Chen, T., Li, E., Jenuwein, T., and Peters, A.H. (2003). Suv39h-mediated histone H3 lysine 9 methylation directs DNA methylation to major satellite repeats at pericentric heterochromatin. Curr Biol 13, 1192-1200.

Liang, G., Chan, M.F., Tomigahara, Y., Tsai, Y.C., Gonzales, F.A., Li, E., Laird, P.W., and Jones, P.A. (2002). Cooperativity between DNA methyltransferases in the maintenance methylation of repetitive elements. Mol Cell Biol 22, 480-491.

Matarazzo, M.R., De Bonis, M.L., Vacca, M., Della Ragione, F., and D'Esposito, M. (2009). Lessons from two human chromatin diseases, ICF syndrome and Rett syndrome. Int J Biochem Cell Biol 41, 117-126.

McGarvey, K.M., Fahrner, J.A., Greene, E., Martens, J., Jenuwein, T., and Baylin, S.B. (2006). Silenced tumor suppressor genes reactivated by DNA demethylation do not return to a fully euchromatic chromatin state. Cancer Res 66, 3541-3549.

McIver, C.M., Lloyd, J.M., Hewett, P.J., and Hardingham, J.E. (2004). Dipeptidase 1: a candidate tumor-specific molecular marker in colorectal carcinoma. Cancer Lett 209, 67-74.

Nan, X., Ng, H.H., Johnson, C.A., Laherty, C.D., Turner, B.M., Eisenman, R.N., and Bird, A. (1998). Transcriptional repression by the methyl-CpG-binding protein MeCP2 involves a histone deacetylase complex. Nature 393, 386-389.

Nguyen, C.T., Weisenberger, D.J., Velicescu, M., Gonzales, F.A., Lin, J.C., Liang, G., and Jones, P.A. (2002). Histone H3-lysine 9 methylation is associated with aberrant gene silencing in cancer

cells and is rapidly reversed by 5-aza-2'-deoxycytidine. Cancer Res 62, 6456-6461.

Ohgane, J., Wakayama, T., Senda, S., Yamazaki, Y., Inoue, K., Ogura, A., Marh, J., Tanaka, S., Yanagimachi, R., and Shiota, K. (2004). The Sall3 locus is an epigenetic hotspot of aberrant DNA methylation associated with placentomegaly of cloned mice. Genes Cells 9, 253-260.

Ohgane, J., Yagi, S., and Shiota, K. (2008). Epigenetics: the DNA methylation profile of tissue-dependent and differentially methylated regions in cells. Placenta 29 Suppl A, S29-35.
Oki, Y., Aoki, E., and Issa, J.P. (2007). Decitabine--bedside to bench. Crit Rev Oncol Hematol 61, 140-152.

Poulaki, V., and Colby, K. (2008). Genetics of anterior and stromal corneal dystrophies. Semin Ophthalmol 23, 9-17.

Rhee, I., Bachman, K.E., Park, B.H., Jair, K.W., Yen, R.W., Schuebel, K.E., Cui, H., Feinberg, A.P., Lengauer, C., Kinzler, K.W., et al. (2002). DNMT1 and DNMT3b cooperate to silence genes in human cancer cells. Nature 416, 552-556.

Rhee, I., Jair, K.W., Yen, R.W., Lengauer, C., Herman, J.G., Kinzler, K.W., Vogelstein, B., Baylin, S.B., and Schuebel, K.E. (2000). CpG methylation is maintained in human cancer cells lacking DNMT1. Nature 404, 1003-1007.

Rodriguez, J., Frigola, J., Vendrell, E., Risques, R.A., Fraga, M.F., Morales, C., Moreno, V., Esteller, M., Capella, G., Ribas, M., et al. (2006). Chromosomal instability correlates with genome-wide DNA demethylation in human primary colorectal cancers. Cancer Res 66, 8462-9468.

Roman-Gomez, J., Jimenez-Velasco, A., Agirre, X., Castillejo, J.A., Navarro, G., San Jose-Eneriz, E., Garate, L., Cordeu, L., Cervantes, F., Prosper, F., et al. (2008). Repetitive DNA hypomethylation in the advanced phase of chronic myeloid leukemia. Leuk Res 32, 487-490.

Roman-Gomez, J., Jimenez-Velasco, A., Agirre, X., Cervantes, F., Sanchez, J., Garate, L., Barrios, M., Castillejo, J.A., Navarro, G., Colomer, D., et al. (2005). Promoter hypomethylation of the LINE-1 retrotransposable elements activates sense/antisense transcription and marks the progression of chronic myeloid leukemia. Oncogene 24, 7213-7223.

Santos-Rosa, H., Schneider, R., Bannister, A.J., Sherriff, J., Bernstein, B.E., Emre, N.C., Schreiber,

S.L., Mellor, J., and Kouzarides, T. (2002). Active genes are tri-methylated at K4 of histone H3. Nature 419, 407-411.

Schneider, R., Bannister, A.J., and Kouzarides, T. (2002). Unsafe SETs: histone lysine methyltransferases and cancer. Trends Biochem Sci 27, 396-402.

Schorderet, D.F., Menasche, M., Morand, S., Bonnel, S., Buchillier, V., Marchant, D., Auderset, K., Bonny, C., Abitbol, M., and Munier, F.L. (2000). Genomic characterization and embryonic expression of the mouse Bigh3 (Tgfbi) gene. Biochem Biophys Res Commun 274, 267-274.

Shah, J.N., Shao, G., Hei, T.K., and Zhao, Y. (2008). Methylation screening of the TGFBI promoter in human lung and prostate cancer by methylation-specific PCR. BMC Cancer 8, 284.

Shao, G., Berenguer, J., Borczuk, A.C., Powell, C.A., Hei, T.K., and Zhao, Y. (2006). Epigenetic inactivation of Betaig-h3 gene in human cancer cells. Cancer Res 66, 4566-4573.

Shiota, K., Kogo, Y., Ohgane, J., Imamura, T., Urano, A., Nishino, K., Tanaka, S., and Hattori, N. (2002). Epigenetic marks by DNA methylation specific to stem, germ and somatic cells in mice. Genes Cells 7, 961-969.

Soengas, M.S., Capodieci, P., Polsky, D., Mora, J., Esteller, M., Opitz-Araya, X., McCombie, R., Herman, J.G., Gerald, W.L., Lazebnik, Y.A., Cordon-Cardo, C. and Lowe, S.W. (2001) Inactivation of the apoptosis effector *Apaf-1* in malignant melanoma. Nature 409, 201-211.

Stoger, R., Kubicka, P., Liu, C.G., Kafri, T., Razin, A., Cedar, H., and Barlow, D.P. (1993). Maternal-specific methylation of the imprinted mouse Igf2r locus identifies the expressed locus as carrying the imprinting signal. Cell 73, 61-71.

Strahl, B.D., and Allis, C.D. (2000). The language of covalent histone modifications. Nature 403, 41-45.

Tachibana, M., Matsumura, Y., Fukuda, M., Kimura, H., and Shinkai, Y. (2008). G9a/GLP complexes independently mediate H3K9 and DNA methylation to silence transcription. EMBO J 27, 2681-2690.

Tachibana, M., Sugimoto, K., Nozaki, M., Ueda, J., Ohta, T., Ohki, M., Fukuda, M., Takeda, N.,

Niida, H., Kato, H., et al. (2002). G9a histone methyltransferase plays a dominant role in euchromatic histone H3 lysine 9 methylation and is essential for early embryogenesis. Genes Dev 16, 1779-1791.

Tachibana, M., Ueda, J., Fukuda, M., Takeda, N., Ohta, T., Iwanari, H., Sakihama, T., Kodama, T., Hamakubo, T., and Shinkai, Y. (2005). Histone methyltransferases G9a and GLP form heteromeric complexes and are both crucial for methylation of euchromatin at H3-K9. Genes Dev 19, 815-826.

Tamaru, H., and Selker, E.U. (2001). A histone H3 methyltransferase controls DNA methylation in Neurospora crassa. Nature 414, 277-283.

Tamaru, H., Zhang, X., McMillen, D., Singh, P.B., Nakayama, J., Grewal, S.I., Allis, C.D., Cheng, X., and Selker, E.U. (2003). Trimethylated lysine 9 of histone H3 is a mark for DNA methylation in Neurospora crassa. Nat Genet 34, 75-79.

Tessema, M., Langer, F., Dingemann, J., Ganser, A., Kreipe, H., and Lehmann, U. (2003). Aberrant methylation and impaired expression of the p15(INK4b) cell cycle regulatory gene in chronic myelomonocytic leukemia (CMML). Leukemia 17, 910-918.

Vermaak, D., Ahmad, K., and Henikoff, S. (2003). Maintenance of chromatin states: an open-and-shut case. Curr Opin Cell Biol 15, 266-274.

Villar-Garea, A., Fraga, M.F., Espada, J., and Esteller, M. (2003). Procaine is a DNA-demethylating agent with growth-inhibitory effects in human cancer cells. Cancer Res 63, 4984-4989.

Warren, S.T. (2007). The epigenetics of fragile X syndrome. Cell Stem Cell 1, 488-489.

Waterston, R.H., Lindblad-Toh, K., Birney, E., Rogers, J., Abril, J.F., Agarwal, P., Agarwala, R., Ainscough, R., Alexandersson, M., An, P., et al. (2002). Initial sequencing and comparative analysis of the mouse genome. Nature 420, 520-562.

Weber, M., and Schubeler, D. (2007). Genomic patterns of DNA methylation: targets and function of an epigenetic mark. Curr Opin Cell Biol 19, 273-280.

Wozniak, R.J., Klimecki, W.T., Lau, S.S., Feinstein, Y., and Futscher, B.W. (2007). 5-Aza-2'-deoxycytidine-mediated reductions in G9A histone methyltransferase and histone H3 K9

di-methylation levels are linked to tumor suppressor gene reactivation. Oncogene 26, 77-90.

Yagi, S., Hirabayashi. K., Sato, S., Li, W., Takahashi, Y., Hirakawa, T., Wu, G., Hattori, N., Hattori, N., Ohgane, J., Tanaka, S., Liu, X.S., and Shiota, K. (2008) DNA methylation profile of tissue-dependent and differentially methylated regions (T-DMRs) in mouse promoter regions demonstrating tissue-specific gene expression. Genome Res 18, 1969-1978

Yang, A.S., Doshi, K.D., Choi, S.W., Mason, J.B., Mannari, R.K., Gharybian, V., Luna, R., Rashid, A., Shen, L., Estecio, M.R., et al. (2006). DNA methylation changes after 5-aza-2'-deoxycytidine therapy in patients with leukemia. Cancer Res 66, 5495-5503.

Yang, A.S., Estecio, M.R., Doshi, K., Kondo, Y., Tajara, E.H., and Issa, J.P. (2004). A simple method for estimating global DNA methylation using bisulfite PCR of repetitive DNA elements. Nucleic Acids Res 32, e38.

Zhu, W.G., Dai, Z., Ding, H., Srinivasan, K., Hall, J., Duan, W., Villalona-Calero, M.A., Plass, C., and Otterson, G.A. (2001). Increased expression of unmethylated CDKN2D by 5-aza-2'-deoxycytidine in human lung cancer cells. Oncogene 20, 7787-7796.

Resistance to 5-aza-2'-deoxycytidine in Genic Regions Compared to

Non-genic Repetitive Sequences

DNA

Epigenetic mechanisms, which involve DNA and histone modifications, result in the heritable silencing of genes without a change in their coding sequence. Study of human diseases have been focused on genetic mechanisms, but expanding studies have shown that disturbance of the balance of epigenetic networks can cause diseases, including cancers, mental retardations and abnormal development. Thus, reversing the abnormal epigenetic alterations has offered a great potential of developing epigenetic drugs in the clinical field. However, such development has overseen the hidden pitfalls regarding the drug usage on patients, mainly on the non-specificity effect on genomic regions and biological mechanisms.

One of the epigenetic drugs, 5-aza-2'-deoxycytidine (5azadC) or decitabine, has recently approved for several malignancies. 5azadC is known to exert its effect by inhibiting DNA methyltranserases (Dnmt), constraining the enzymatic activities and results in unmethylated DNA after several replications. There are several kinds of Dnmts, each has specific preference on genomic regions. Besides, growing evidence shows direct linking of histone modification enzymes to DNA methylation and Dnmt to histone modifications. These have raised concerns on its inducing effects, in addition to DNA demethylation.

This thesis addresses questions regarding the potential of 5azadC to induce non-targeted effect on different genomic regions and on other epigenetic modifications. Understanding of such behind mechanisms is imperative to develop better therapies for disease treatment.

89

Chapter 1 – Resistance of Genic Regions against 5-aza-2'-deoxycytidine Compared to Non-genic Repetitive Sequences

5-aza-2'-deoxycytidine (5azadC) has been widely used as a Dnmt inhibitor to reverse aberrant hypermethylation. 5azadC exerts its demethylating effect by covalently binding to Dnmts. As Dnmts have multi targets, there is potential of causing genome-wide demethylating effect by using 5azadC and risk of demethylating non-targeted genomic regions might occur. In addition, there are diverse interactions between DNA methylation and histone modification in euchromatic and heterochromatic regions. Possibility to induce hypomethylation-independent activation of gene expression and downstream responses might exist. This chapter studies the effect of 5azadC on non-genic repetitive sequences and some genic regions including T-DMRs.

Considering the potential effect of 5azadC on non-targeted genomic regions in normal cells, i investigated its effect on repetitive sequences and selected gene loci, *Oct-4*, *Sall3*, *Per1*, *Clu*, *Dpep1* and *Igf2r*, including tissue-dependent and differentially methylated regions, by treating mouse NIH/3T3 fibroblast cells with concentrations of 5azadC ranging from 0.001 μM to 5 μM. Demethylation of minor satellite repeats and endogenous viruses was concentration dependent, and they were strongly demethylated at 1 and 5 μM. In genic regions, methylation level decreased only at 0.1 μM, but was minimally altered at concentrations lower or higher, regardless of the abundance of CpG sites. Thus, repeats are strongly demethylated, but genic regions are only demethylated at effective doses.

Genes were activated by 5azadC treatment, and were accompanied by a unique combination of histone modifications in genic regions, including an increased level of H3K9me3 and a decreased level of AcH3. Increase of H3K9me3 in genic regions was not observed in Dnmt knock out cells. I identified differential effects of 5azadC on repetitive sequences and genic regions, and revealed the importance of choosing appropriate 5azadC doses to achieve targeted gene recovery and to minimize side effects in patients receiving cancer treatment.

Chapter 2 – Epigenetic Regulation in *Tgfbi*

Transforming growth factor beta-induced gene (*Tgfbi*) is associated with corneal development and healing, adhesion and spreading of fibroblast and tumor suppressor activity. Mutations in *Tgfbi* have caused different kinds of cornea dystrophies. Recent studies have revealed epigenetic defects in *Tgfbi*, in association in several kinds of cancers. This chapter studies various epigenetic mechanisms controlling *Tgfbi*, and epigenetic therapy in treating deregulation of *Tgfbi* is anticipated.

5azadC induced demethylation of hypermethylated regions of *Tgfbi* in NIH/3T3 cells. Similar to those in Chapter 1, the regions were resistant to demethylation at 1 μM compared to 0.1 μM of 5azadC, but CpG island was demethylated by both concentrations. 5azadC induced increment of H3K9me3 and a reduced level of H3K9me2. Increased of H3K4 marks corresponded to gene

upregulation.

In Dnmt knock out cells, DNA methylation of *Tgfbi* was severely depleted. A complete loss of methylation was observed in *Dnmt3a$^{-/-}$3b$^{-/-}$*, and was accompanied by increased H3K9me2 and a drastic decrease of H3K9me3 in *Tgfbi*. In *Dnmt1$^{-/-}$* cells, a moderate level of DNA methylation remained, H3K9me3 level was maintained and H3K9me2 was decreased. Together with 5azadC results, these suggested the role of H3K9me3 in DNA methylation maintenance.

Histone H3K9 methyltransferase *G9a* deficient cells had a reduced DNA methylation level in *Tgfbi* compared to wild type, and the DNA methylation level was further reduced following Dnmt1 knock down. In contrast, *Suv39h* deficient did not affect DNA methylation level. Taken together, DNA methylation maintenance in *Tgfbi* involves both Dnmts and G9a, and that 5azadC-induced demethylation resistance might involve complicated changes governed by these enzymes.

Discussion

Current studies provide evidence that 5azadC has different impact on DNA methylation between non-genic regions and genic regions. Non genic repetitive sequences were strongly demethylated by 5azadC, but genic regions were only demethylated at particular concentrations and were minimally affected by higher dosage.

5azadC does not only affect DNA methylation, but also alter histone modifications with unusual combination. Of this combination of histone modifications, H3K9me2 decreased followed by increase of H3K9me3 maybe responsible for resistance of genic regions to 5azadC-demethylating activity. Since changes of H3K9me2/H3K9me3 were not observed in *G9a* deficient cells, and DNA methylation was reduced in *G9a* deficient cells and was further reduced by *Dnmt1* knock down, implying that G9a is involved in 5azadC resistance mechanisms.

**Resistance to 5-aza-2'-deoxycytidine in Genic Regions Compared to
Non-genic Repetitive Sequences**

DNA

5azadC   decitabine

5azadC   DNA   Dnmt

DNA   DNA

Dnmt

DNA   DNA

Dnmt

5azadC

5azadC

5azadC   Dnmt

5azadC   Dnmt   Dnmt

5azadC

DNA

DNA

T-DMR

5azadC

5azadC

T-DMR   6   Oct-4, Sall3, Per1, Clu, Dpep1, Igf2r

NIH/3T3   5azadC   0.001μM   5μM

1μM   5μM

5azadC   0.1μM

CpG

5azadC

5azadC

H3K9me3   AcH3

Dnmt   H3K9me3

5azadC

5azadC

Tgfbi

Tgfbi

Tgfbi

Tgfbi

Tgfbi

Tgfbi

NIH/3T3　　　　　　　　5azadC　　Tgfbi

1　　　　　　5azadC　　　0.1μM　　　　　　　　　1μM

CpG

5azadC　　　　H3K9me3　　　　　　　　　　　　　　H3K9me2

H3K4

Dnmt　　　　　　　Tgfbi　　DNA

Dnmt3a-/-3b-/-　　　　Tgfbi　　　　　　　　　　　　　　H3K9me2

H3K9me3　　　　　　　　　　　　　Dnmt1-/-　　　DNA

H3K9me3　　　　　　　H3K9me2

DNA　　　　　　　　H3K9me3

H3K9　　　　　　　　G9a

Tgfbi　DNA　　　　　　　　　　　　　　　　G9a　　　　　Dnmt1

DNA　　　　　　　　　　　　　　　　Suv39h

DNA　　　　　　　　　　　　　　　　　　　　Tgfbi

DNA　　　　　Dnmt　G9a　　　　　　　5azadC

5azadC　DNA

5azadC

5azadC

5azadC　DNA

H3K9me2　　　　　　　　H3K9me3　　　5azadC

G9a　　　　H3K9me2/H3K9me3

DNA　　　　　　　Dnmt1

DNA　　　　　　　　　G9a　5azadC